

AD-A064 753

AIR FORCE INST OF TECH WRIGHT-PATTERSON AFB OHIO SCH--ETC F/G 20/12  
DEPTH-RESOLVED CATHODOLUMINESCENCE OF CARBON IMPLANTED GALLIUM --ETC(U)  
DEC 78 L V PARZIANELLO  
AFIT/GEP/PH/78D-9

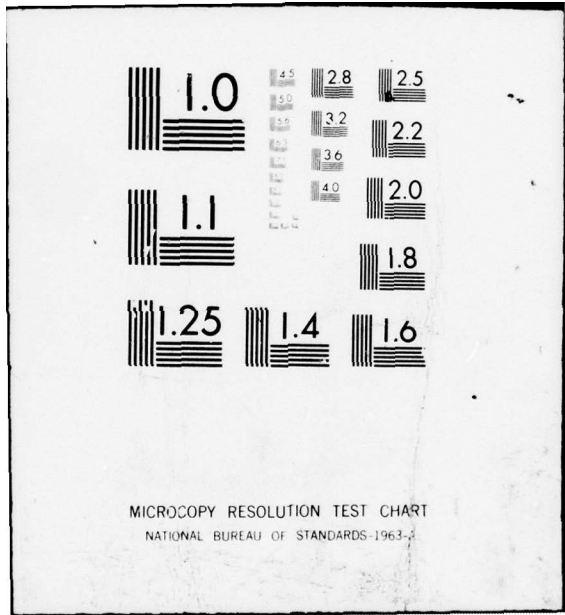
UNCLASSIFIED

NL

1 OF 1  
AD 64753



END  
DATE  
FILMED  
4--79  
DDC



ADA064753

LEVEL

15

# AIR FORCE INSTITUTE OF TECHNOLOGY



AIR UNIVERSITY  
UNITED STATES AIR FORCE

DDC FILE COPY



DDC  
FEB 22 1979

AQT

## SCHOOL OF ENGINEERING

DISTRIBUTION STATEMENT 1  
Approved for public release  
Distribution Unlimited

WRIGHT-PATTERSON AIR FORCE BASE, OHIO

79 01 30 166

LEVEL II

①

ADA064753

DDC FILE COPY

1048970

DEPTH-RESOLVED CATHODOLUMINESCENCE  
OF CARBON IMPLANTED GALLIUM ARSENIDE

THESIS

AFIT/GEP/PH/78D-9

Luciano V. Parzianello  
Captain USAF

DDC  
RECEIVED  
FEB 22 1979

6 DEPTH-RESOLVED CATHODOLUMINESCENCE  
OF CARBON IMPLANTED GALLIUM ARSENIDE

9 Master's thesis  
THESIS

Presented to the Faculty of the School of Engineering  
of the Air Force Institute of Technology  
Air University  
in Partial Fulfillment of the  
Requirements for the Degree of  
Master of Science

12 66 p.

16 2386

17 R2

by

10 Luciano V. Parzianello

Captain USAF

Graduate Engineering Physics

11 December 1978

|                              |           |
|------------------------------|-----------|
| SEARCHED                     | INDEXED   |
| SERIALIZED                   | FILED     |
| JAN 1979                     |           |
| AFIT                         |           |
| DISTRIBUTION STATEMENT CODES |           |
| FORM                         | MAIL ROOM |
| A                            |           |

Approved for public release; distribution unlimited.

012 225

elf

## Preface

The completion of this thesis was a very gratifying experience, and I would like to express my gratitude to those persons who assisted me in this endeavor. I am grateful to my advisor, Dr. Robert L. Hengehold, who steered me in the right directions. The thesis was sponsored by the Air Force Avionics Laboratory/DHR, and I would like to thank this organization for providing the ion implanted samples which were the centrum of the thesis. I would also like to thank my fellow students, Captains Ronald L. Lusk and James H. Walcher, who frequently provided insight into the burning questions of the day. The technical assistance provided by Ron Gabriel, George Gergal and Jim Miskimen of the AFIT Physics Laboratory staff was also appreciated. Finally, I would also like to acknowledge my appreciation for my family's understanding of my conspicuous absences during this period of study.

Luciano V. Parzianello

(This thesis was typed by Sharon A. Gabriel)

Table of Contents

|  | Page |
|--|------|
| Preface.....                             | ii   |
| List of Tables and Figures.....          | iv   |
| Abstract.....                            | vi   |
| I. Introduction.....                     | 1    |
| II. Theory and Previous Work.....        | 4    |
| Ion Implantation.....                    | 4    |
| Luminescence.....                        | 6    |
| Energy Peak Shifts.....                  | 12   |
| Cathodoluminescence Model.....           | 18   |
| III. Results and Discussion.....         | 26   |
| Luminescence Peak Energies.....          | 28   |
| Peak Energy Shifts.....                  | 43   |
| Cathodoluminescence Model.....           | 45   |
| IV. Conclusions and Recommendations..... | 48   |
| Conclusions.....                         | 48   |
| Recommendations.....                     | 49   |
| Bibliography.....                        | 51   |
| Vita.....                                | 54   |

List of Tables and Figures

| <u>Table</u>      |   | <u>Page</u> |
|-------------------|---|-------------|
| I                 | Sample Numbering and Preparation Conditions.....  | 29          |
| <br><u>Figure</u> |   |             |
| 1                 | The Standard LSS Profile for Carbon Implanted in GaAs with Fluence of $10^{13}$ ions/cm <sup>2</sup> at an Implant Energy of 120 KeV (Ref. 17)..... | 7           |
| 2                 | Energy Band Diagram - Simple Centers.....   | 8           |
| 3                 | Dependence of Spectral Peak Positions of GaAs Band Edge Emissions on Doping for Both 77° K and 300° K (Ref. 2).                                     | 13          |
| 4                 | Cathodoluminescence Spectra of Zn-doped GaAs at 4.2° K (Ref. 2).....  | 14          |
| 5                 | Model for Radiative Recombination Between Donors and Residual Acceptors in n-type GaAs (Ref. 31).....   | 15          |
| 6                 | Peak Photon Energy Vs. Peak Light Intensity for a Compensated GaAs Sample (Ref. 31).....  | 17          |
| 7                 | Tunneling-Assisted Emission in Compensated GaAs at Low and High Excitation Rates (Ref. 31).....   | 18          |
| 8                 | Smoothed Energy Loss Curves for Electrons Incident on GaAs at 45° (Ref. 17).....  | 23          |
| 9                 | Theoretical L(V) Curve for Carbon-Ion Implant of $10^{13}$ ions/cm <sup>2</sup> at Implant Energy of 120 KeV into GaAs (Ref. 17).....               | 24          |
| 10                | Cathodoluminescence System Diagram (Ref. 14).....   | 27          |
| 11                | Typical Spectrum for Sample 34.....   | 30          |
| 12                | Typical Spectrum for Sample 36.....   | 31          |
| 13                | Typical Spectrum for Sample 37.....   | 32          |
| 14                | Spectrum of Sample 34 Taken at 39° K.....   | 34          |
| 15                | Spectrum of Sample 34 - Three Peaks.....  | 35          |
| 16                | Spectra for Sample 34 at Different Beam Voltages.....   | 40          |



List of Tables and Figures (Cont'd)

| <u>Figure</u> |  | <u>Page</u> |
|---------------|--|-------------|
| 17            | Spectra for Sample 34 at Different Beam Currents.....  | 41          |
| 18            | Spectra for Sample 37 at Different Beam Voltages.....  | 42          |
| 19            | Theoretical L(V) Curve Vs. Experimental L(V) Curve, for<br>Carbon-ion Implant of $10^{13}$ ions/cm <sup>2</sup> and at Implant Energy<br>of 120 KeV into GaAs..... | 47          |

Abstract

Three samples of VPE GaAs grown on SI Cr compensated substrate were examined by depth resolved cathodoluminescence using electron beam energies from 2.5 KeV to 15 KeV at 10° K and 39° K. The samples had been carbon-implanted, at a 120 KeV implant energy, with fluences of  $10^{13}$  ,  $10^{14}$  and  $10^{15}$  carbon ions/cm<sup>2</sup> , respectively. The resulting cathodoluminescent spectra contained eight energy peaks: an unresolved exciton peak at 1.514 eV, a conduction band-to-carbon acceptor peak at 1.494 eV, a carbon donor-to-carbon acceptor peak at 1.490 eV, a possible carbon donor-to-zinc acceptor peak at 1.487 eV, two optical phonon peaks at 1.457 eV and 1.454 eV, an unresolved As vacancy complex at 1.408 eV, and, finally, an unresolved Ga vacancy complex or  $As^+ Cu^- A^+$  complex at 1.361 eV.

An attempt was made to observe impurity concentration dependent energy peak shifts, of the conduction band-to-carbon acceptor and the carbon donor-to-carbon acceptor energy peaks, which had been reported for carbon implanted bulk-grown GaAs and attributed to carbon impurity banding. The failure to observe energy peak shifts in the higher-purity VPE GaAs indicates that a more probable explanation for the peak shifts observed in the bulk-grown GaAs involves the use of a tunneling-assisted transition model which considers the combined effects of the implanted carbon impurity and the compensating impurity, Cr, present in the bulk-grown GaAs.

Finally, the cathodoluminescence spectral data was compared to the theoretical predictions of a cathodoluminescence model for GaAs

developed by M. L. Cone in his Doctoral Dissertation. It was concluded that more experimental data is required to make an objective comparison.

DEPTH-RESOLVED CATHODOLUMINESCENCE  
OF CARBON IMPLANTED GALLIUM ARSENIDE

I. Introduction

The United States Air Force is currently interested in developing semiconductor devices which must operate in high-temperature environments and at high microwave frequencies. One binary semiconductor, gallium arsenide (GaAs), is expected to provide, with proper impurity doping, the desired characteristics for developing such devices.

Gallium arsenide is a binary semiconducting III-V compound which crystallizes in the zincblende crystal structure. Although its physical properties are very similar to the covalent bond group-IV semiconductors such as silicon and germanium, the slightly ionic bonding in GaAs results in its higher electron mobilities. The location of gallium and arsenic in the periodic table leads to a wider band gap energy for GaAs than for silicon and germanium (Ref. 15:371-372). These properties of GaAs, coupled with proper doping, make this semiconductor ideal for developing the required Air Force devices.

For years now, the Air Force Avionics Laboratory, Wright-Patterson Air Force Base, Ohio, has been conducting research on ion implantation as a doping method for GaAs. Ion implantation or the introduction of energetic ionized atoms into a substrate, with resulting changes in the substrate's electrical, metallurgical or chemical properties, has been extensively used in silicon semiconductor studies (Ref. 16:151-249). The advantages provided by ion implantation include accurate control

of the amount of ions or impurities transferred to the substrate and greater control of impurity density and profile in the substrate. However, not as much is known about ion implantation in GaAs and even less about carbon-ion implants in GaAs. More information is needed about how carbon is deposited in GaAs, how active it is optically, what defects it introduces into the GaAs substrate.

One method by which the properties of an ion implanted species can be studied is that of luminescence. Luminescence is that process by which a portion of the excitation energy absorbed by a material is emitted in the form of light radiation. If the excitation energy is provided by an electric current, the light emission is called electroluminescence, whereas if the excitation is optical, the emission is referred to as photoluminescence. When the excitation energy is provided by a beam of energetic electrons, accelerated by a potential, the emission from the material is called cathodoluminescence. Since the depth to which the electrons penetrate into the material depends on their initial kinetic energy or accelerating potential, the electrons can be made to excite or probe different depths of the material by varying the accelerating potential. This process is called depth-resolved cathodoluminescence. The process of cathodoluminescence, in various forms, has been used to analyze and characterize different materials and, specifically, semiconductors (Ref. 1-14). Its use provides a nondestructive method of characterizing semiconductors and provides information about impurity profiles and defects in semiconductor materials which have been ion-implanted with various known impurities.

The purpose of this study was threefold: first, to analyze previous cathodoluminescence data from carbon-ion implanted GaAs,

obtained by students and staff members of the Physics Department, Air Force Institute of Technology, Wright-Patterson AFB, Ohio, and to obtain additional selective data; second, to study and attempt to explain energy peak shifts observed in the cathodoluminescent spectra of certain carbon implanted GaAs samples; and, lastly, to determine if the cathodoluminescence model developed by Cone (Ref. 17) would fit the data obtained for carbon-ion implanted GaAs.

In the theory and previous work section of this thesis, ion-implantation, luminescence processes, background work, energy peak or band shifts, and the cathodoluminescence model are discussed. The results and discussion section includes a brief discussion of the cathodoluminescence system and an analysis of previous and current data with emphasis on identification of energy peaks or bands in light of results and the literature. The conclusions and recommendations section presents both conclusions drawn from this work and recommendations about what could be improved in the present procedures and what future work should include.

## II. Theory and Previous Work

This chapter contains the background theory and results of previous work which are necessary to understand and explain the experimental results. The major headings covered are: ion-implantation, luminescence by radiative recombination, energy peak shifts, and the cathodoluminescence model developed by Cone (Ref. 17).

### Ion Implantation

Since the samples analyzed for this thesis and previous work are based on ion-implanted GaAs, it is appropriate to briefly discuss ion-implantation and the resulting impurity density profile predicted by LSS theory. The density profile or LSS profile will again be discussed in the section pertaining to the cathodoluminescence model developed by Cone.

Ion-implantation is the introduction of energetic ionized atoms into a substrate, with resulting changes in the substrate's electrical, metallurgical or chemical properties. As the substrate is struck by the beam of energetic ions, the substrate will lose some of its own atoms by sputtering, but it will also retain a certain amount of the incident ions. The amount of incident ions retained by the substrate have, therefore, been ion-implanted and the theory of Lindhard, Scharff and Schiott (LSS) predicts the spatial distribution of the implanted ions in the substrate.

The implanted ions will lose their energy through interactions of the ions with the electrons in the substrate and with collisions of the ions with the nuclei of the target. Since all the ions do not

come to rest or lose all their energy at the same depth, a distribution is obtained, about some average depth, which is called the projected range. Assuming a Gaussian spatial distribution for the implanted ions and taking into account both electron collisions and nuclear collisions, the LSS theory predicts the following ion density in the substrate:

$$n(x) = \frac{F}{(2\pi)^{\frac{1}{2}} \Delta R} e^{-\left[\frac{x - R}{(2)^{\frac{1}{2}} \Delta R}\right]^2}$$

where

- F = dose (i.e., total number of ions per unit area striking the substrate's surface)
- R = projected range of the ions into the substrate in a direction perpendicular to the substrate's surface
- $\Delta R$  = standard deviation of the projected range R
- x = distance into the substrate in a direction perpendicular to the substrate's surface
- n(x) = density of implanted ions (i.e., total number of ions per unit volume which have stopped at a distance x into the substrate)

The values for R and  $\Delta R$  will depend on the initial kinetic energy of the implanted ions, the mass of the ions, and the mass or density of the substrate. Methods for calculating values for R and  $\Delta R$  and the details for arriving at the expression for n(x) are clearly described in a lengthy work by Gibbons (Ref. 34). It is felt that further discussion of the theory is beyond the scope of this thesis.



What the expression for  $n(x)$  indicates, however, is that the majority of ions will be deposited at a distance  $x = R$  and the remainder will be distributed symmetrically about  $R$  in a Gaussian distribution with the density dropping by one decade at  $x \approx R \pm 2 R$  (Ref. 34:304). A computer generated plot of the LSS density profile for a carbon-ion implant, at an energy of 120 KeV and a dose of  $10^{13}$  carbon ions per square centimeter, into a GaAs substrate is shown in Figure 1.

The LSS profile provides a very good prediction of the density distribution of carbon implanted into GaAs. In a current work, Shin (Ref 41:438) states that electrical profiling studies of carbon implanted GaAs show that the density profiles follow closely the LSS carbon-ion profile, indicating that the diffusion of carbon is negligible at least up to annealing temperatures of  $900^{\circ} C$ .

#### Luminescence

When a semiconductor material such as GaAs is excited by a beam of energetic electrons, cathodoluminescence occurs. This luminescence, in its simplest form, is a result of the radiative recombination of electron-hole pairs which were generated by the energetic electron beam. The radiative recombinations will often involve both simple and complex optically active centers which complicates the interpretation of luminescent data.

Examples of simple center radiative recombinations include conduction band-valence band, free exciton, band-impurity, and impurity-impurity. Boulet (Ref. 11:4-8) presents a detailed explanation of the

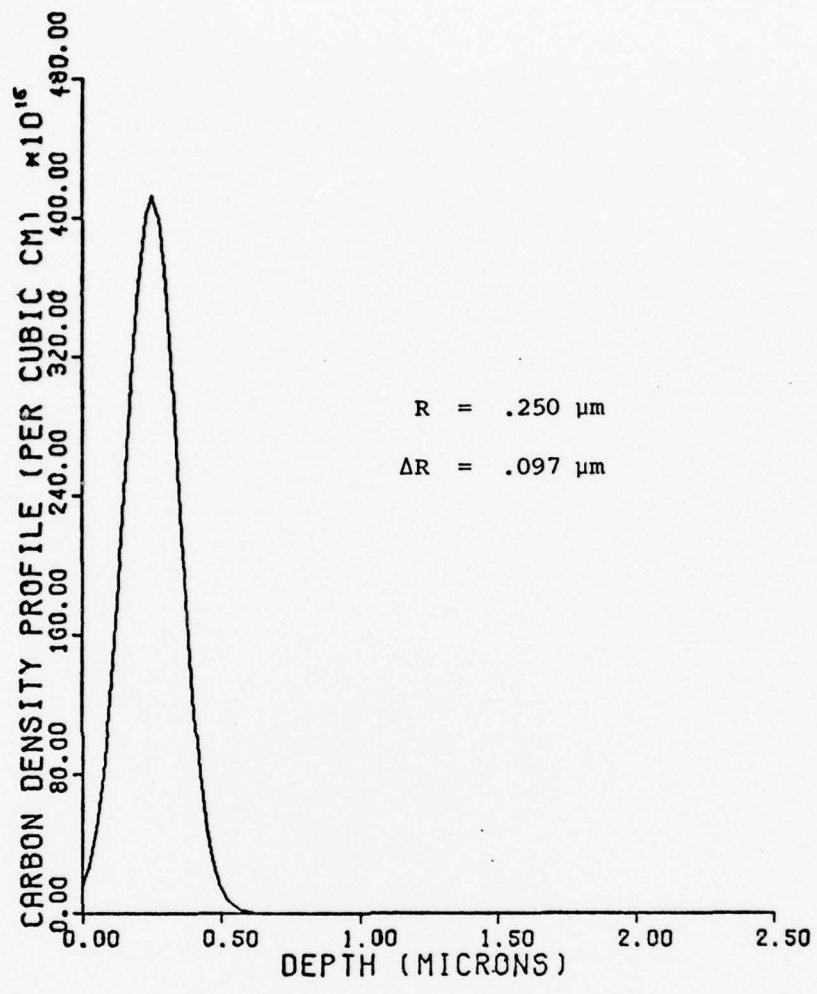


Figure 1. The Standard LSS Profile for Carbon Implanted in GaAs with Fluence of  $10^{13}$  ions/cm<sup>2</sup> at an Implant Energy of 120 KeV. (Ref. 17)

recombinations and Figure 2 illustrates an energy band diagram with the simple center recombinations mentioned.

The band gap energy,  $E_g$ , for GaAs is taken as 1.521 eV at 10° K (Ref. 18:770). When an electron in the conduction band recombines with a hole in the valence band, a band-band recombination occurs with an energy equal, at minimum, to the band gap energy.

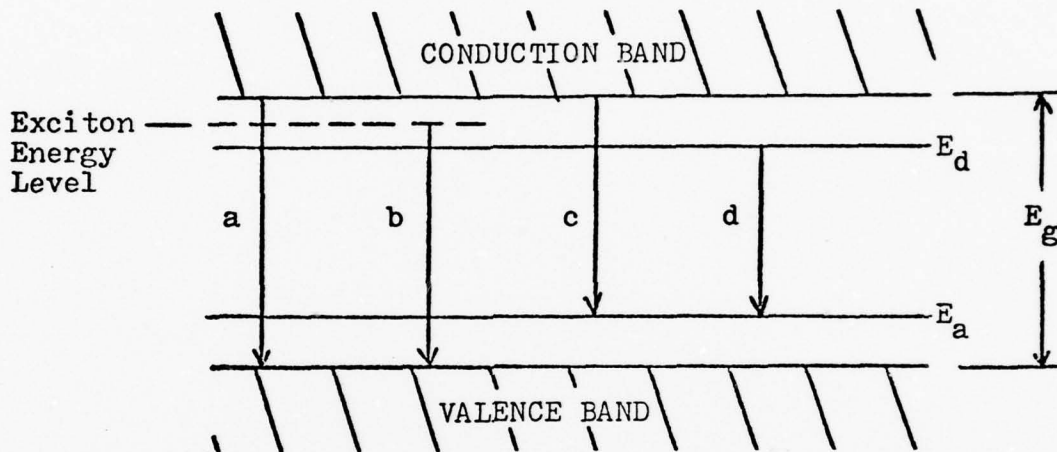


Figure 2. Energy Band Diagram - Simple Centers

- a) Band-Band
- b) Free Exciton
- c) Band-Impurity
- d) Impurity-Impurity

Free excitons involve an electron bound to a hole in a hydrogen-like manner and they are free to move through the lattice. Because of the coulombic binding energy, when the electron and hole recombine, the energy emitted will be slightly less than  $E_g$  (Ref 19:332-334).

The band-impurity or free-bound recombination involves the recombining of a free electron (hole) with a hole (electron) bound to an impurity with the transition having an approximate energy

$$E = E_g - E_i + \bar{E}_k \pm nE_p$$

where  $E_i$  is the donor or acceptor impurity binding energy,  $\bar{E}_k$  is the average kinetic energy of the electron/hole, and  $E_p$  is the optical phonon with  $n$  being a positive integer or zero.

The impurity-impurity or donor-acceptor transition involves the recombination of an electron bound to a donor impurity with a hole bound to an acceptor impurity. If the separation,  $R$ , between the donor and acceptor is large compared with the radii of the unperturbed donor and acceptor atoms, the donor-acceptor transition energy is approximated by (Ref. 20:13)

$$E = E_g - E_a - E_d + e^2/kR \pm nE_p$$

where  $E_a$  is the acceptor binding energy,  $E_d$  is the donor binding energy,  $R$  is the separation,  $e^2/kR$  is the coulomb interaction term between the donor and acceptor atoms, and the last term is added for the optical phonon energy. Since the radiative recombination rate varies approximately as the negative exponent of the separation  $R$  (Ref. 20:85), the more distant donor-acceptor pairs (large  $R$ ) are saturated before the near pairs and the net contribution from the near pairs increases the value of the  $e^2/kR$  term. Hence, an increase in excitation intensity saturates the distant pairs, while the near pairs which recombine at a faster rate dominate the transition process resulting in an increase of the donor-acceptor transition peak energy.

A brief discussion of complex radiative recombination centers, which involve a deep level impurity or a vacancy complex, is now presented. The subject of vacancy complexes has received considerable attention as evidenced by the literature, but firm agreement is lacking as to the correct complex center responsible for various luminescence bands observed in GaAs. Two luminescent bands occurring at 1.40 eV and 1.35 - 1.37 eV have been attributed to different complexes. Demoulin states that, in general, for almost all complex luminescent bands, impurity doping studies have indicated that the impurity is responsible for the luminescent band, while temperature annealing studies have indicated that vacancies are responsible (Ref. 12:7).

This maxim is exemplified by the 1.40 eV band studies by various researchers. Demoulin cites studies on GaAs crystals doped with Mn which convinced some researchers that the 1.41 eV band was due to the Mn impurity since the Mn doping resulted in a band, or greatly enhanced an already existing one, at 1.41 eV (Ref. 21:54, 22:3062). On the other hand, studies of undoped GaAs annealed under different conditions indicated the 1.41 eV band was due to vacancies (Ref. 23:144, 24). Chang et al. (Ref. 23) were able to show that the 1.40 eV band could be suppressed with an As overpressure during annealing in sealed quartz ampoules. They inferred the 1.40 band is most probably due to As vacancy complexes.

The same ambivalence applies to the popular 1.35 - 1.37 eV luminescent band. Chang et al. in the same study mentioned above, related the dependence of the 1.35 eV band to Ga vacancies by observing

its dependence upon As overpressure during annealing, while relating a sharp band at 1.37 eV to the intentional doping with copper, of various crystals. Queisser and Fuller (Ref. 25) identify a Cu acceptor on a Ga site with a band at 0.155 eV above the valence band, or 1.37 eV, after doping GaAs with copper. A more recent study by Guislain, DeWolf and Clauws (Ref. 26) performed a comprehensive comparison of the 77° K photoluminescent spectra of about one hundred n-type GaAs single crystals grown either by the horizontal or by the Czochralski technique. They found that the principle native defects in crystals grown by the horizontal method (in the as-grown state) are As vacancies, whereas Ga vacancies are the dominant native defects in crystals grown by the Czochralski technique. One of their conclusions is that the complex center yielding the 1.35 eV band (a broad band), usually identified as substitutional copper (on a Ga site), has to be defined as the As vacancy associated defect complex,  $V_{As}^+ Cu^- V_{As}^+$ , in order to fit all the experimental data. In this study, the authors also state the essential fact that copper is known to be the most frequently introduced acceptor contaminant and is believed to originate from the quartzware (ampoules, boats, etc.). They go on to say that it appeared that the whole spectrum was very sensitive to the thermal history of the crystal during its growth and, consequently, none of the observed peaks could be used alone as a reference for copper contamination. The fact of As vacancies being dominant in horizontal boat-grown GaAs is supported in part by a study by Chiang and Pearson (Ref. 27) in which they report that two types of defects were introduced as the result of annealing. These have been identified, by As vapor pressure dependencies,

as As vacancies having a high surface concentration and acting as donors, and Ga vacancies acting as acceptors having a lower surface concentration but extending further into the crystal. One of the key facts brought out is that, in two of the three different grades of quartz used for heat treatment ampoules, copper contamination from the quartz masked the vacancy diffusion toward the surface.

In summation, complex centers offer a wide latitude for interpretation and, in order to continue with the present work, it was assumed after an extensive literature search that the most probably cause for the 1.40 eV band is an As vacancy-acceptor complex, and that the 1.35 - 1.37 eV band is due to either copper contaminants on Ga sites or to the more elaborate  $\text{As}^+ \text{Cu}^- \text{As}^+$  complex. The question of whether copper takes a prominent role in this band is very essential to the cathodoluminescent model developed by Cone, which will be discussed shortly.

#### Energy Peak Shifts

In previous work, Walter (Ref. 14:7-11) discusses the concentration dependence of luminescence when the concentration of an impurity reaches a density where the electronic wave functions of the impurities overlap and the impurity begins to form energy bands. This banding has been shown to cause a shift in band-impurity and impurity-impurity luminescent peaks in GaAs (Refs. 2, 4). For n-type GaAs, banding is believed to begin at a carrier concentration of about  $5 \times 10^{16}/\text{cm}^3$  with merging of this impurity band with the conduction band at about  $1 \times 10^{17}/\text{cm}^3$ . For simple hydrogenic acceptors (p-type GaAs), the banding begins at about  $5 \times 10^{17}/\text{cm}^3$  and merging with the valence band begins at about 2 or  $3 \times 10^{18}/\text{cm}^3$  (Ref. 28:358).

By probing samples 1, 2, 3 and 4 (see Table I, this work) with varying electron beam energy, Walter observed definite shifts to higher energies as the probing passed through the peak impurity concentration, where banding would be maximum, and then to depths where impurity concentration drops off and banding decreases with a corresponding increase in the impurity-impurity transition energy peak (Ref. 14:46-49).

Based on this model of banding, Walter deduced donor and acceptor concentrations from the work by Cusano (Ref. 2) in which some results of the dependence of spectral peak positions of GaAs band edge emissions on doping were summarized for various dopants. Those results are illustrated in Figure 2.

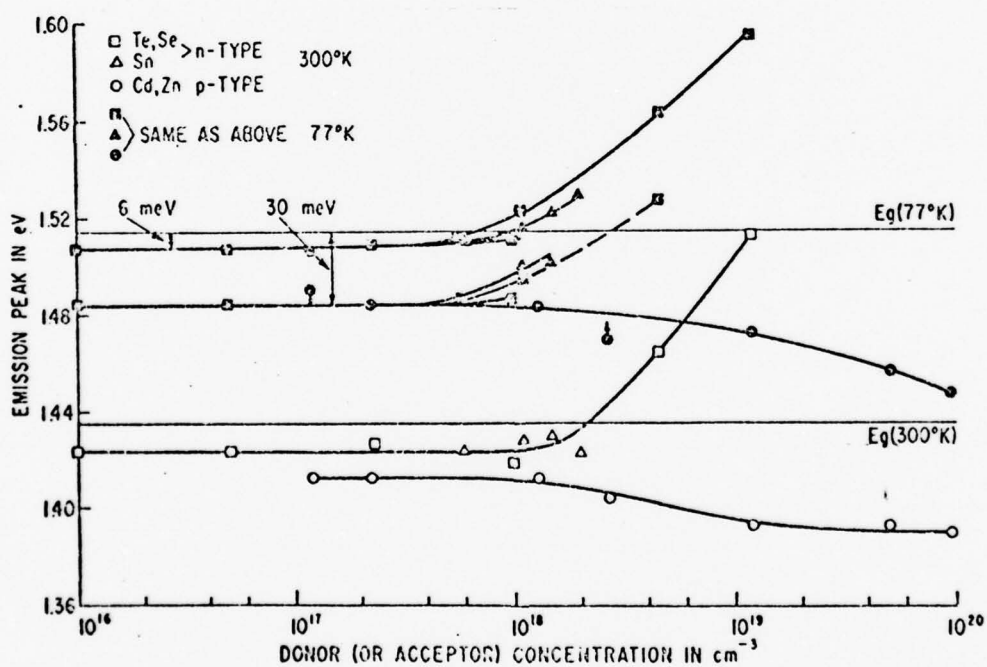


Figure 3. Dependence of Spectral Peak Positions of GaAs Band Edge Emissions on Doping for Both 77° K and 300° K (Ref. 2)



The dependence of both the spectral line shape and peak position for Zn-doped GaAs at 4.2° K were also observed by Pankove and are shown in Figure 3 (Ref. 4:298). The spectra clearly indicate a shift to lower energies as banding of the Zn impurity apparently has occurred. Based on these observations, Walter was able to estimate donor or acceptor concentrations.

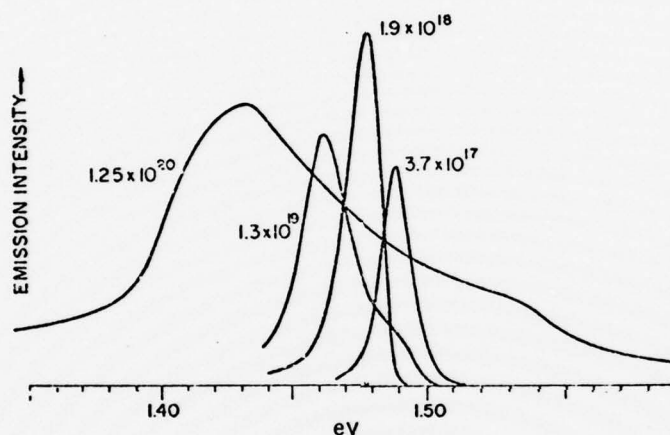


Figure 4. Cathodoluminescence Spectra of Zn-doped GaAs at 4.2° K (Ref. 4)

Due to the variance of Walter's results with the results of subsequent work and this thesis, it was felt that another explanation was necessary to describe the results. One explanation which Walter did not consider involves considering the combined effect of both the carbon implanted impurity and the chromium, Cr, impurity present in the GaAs as a compensator (approximately  $10^{16} - 10^{17}$  Cr atoms per cubic centimeter). What now follows is a proposed explanation for the variance in results.

First, I will discuss how the carbon impurity can form band tails or density of states tails on the conduction band edge. These band tails are formed when the conduction band edge is perturbed by the coulomb interaction of the ionized carbon donor, or by the deformation potential brought about by the fact that the impurity, carbon in this case, is smaller than an atom (Ga or As) of the host lattice and, therefore, produces a local mechanic strain (Ref. 31:10-12). Both of these effects allow electronic energy states to extend from the conduction band edge into the forbidden region. Wherever these situations occur, the conduction band edge is perturbed and band tail states are formed. These effects could also occur with acceptor impurities with a subsequent perturbation of the valence band edge and formation of band tail states on the valence band. As stated already, a donor impurity such as carbon in GaAs can form band tails on the conduction band edge and a model for this is illustrated by Pankove (Ref. 31) in Figure 5 below.

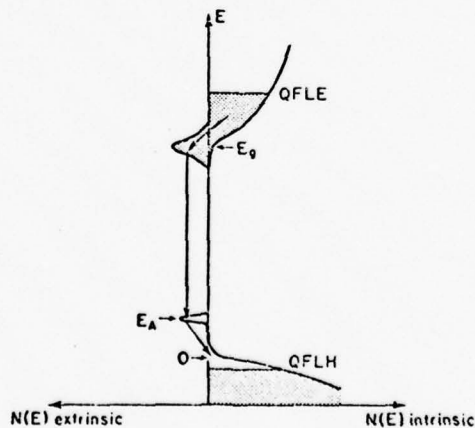


Figure 5. Model for Radiative Recombination Between Donors and Residual Acceptors in n-type GaAs (Ref. 31)

In a cathodoluminescent study of moderately and heavily doped n-type GaAs (Ref. 5), Pankove discusses this model. As shown in Figure 5, in moderately doped n-type GaAs the donor tail states overlap the tail of the conduction band. Pankove states the acceptor levels are about 30 meV above the valence band. As the quasi-Fermi level for holes moves deeper into the valence band under increased excitation, a donor-to-valence-band transition would be expected to produce an emission spectrum with an energy at about  $E_g - E_D$  and the emission peak would shift to higher energies. However, no shift was observed and the emission peak in moderately doped n-type GaAs occurred at about  $E_g - 30 \text{ meV} = E_g - A_A$ . Pankove interpreted this behavior as a donor-to-acceptor radiative transition, which is independent of the position of the quasi-Fermi levels. Similar results were obtained by Pankove for moderately doped p-type GaAs (Ref. 4). Hence, consideration of only the carbon implant does not give a complete explanation of the peak energy shift in light of Pankove's findings.

However, Pankove then considered the case of closely compensated GaAs and proposed another model to describe observed results of the peak shift (Ref. 31:149-152). He reports that in contrast to the above described behavior of moderately and heavily doped samples, in closely compensated GaAs the emission spectrum shifts to higher energies as the excitation rate increases. He states that such shifts are observed under electron-beam excitation as well as under photoluminescence. As shown in Figure 6, the energy of the emission peak of closely compensated n-type GaAs increases logarithmically with the emission intensity and nearly logarithmically with the excitation rate.

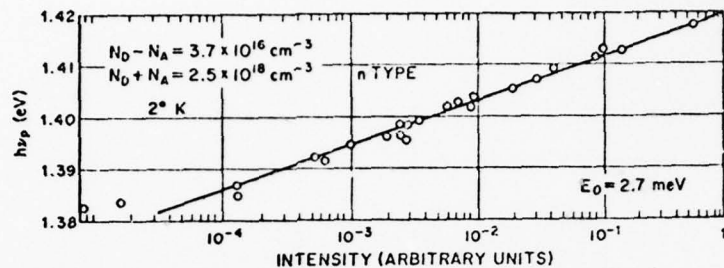


Figure 6. Peak Photon Energy Vs. Peak Light Intensity for a Compensated GaAs Sample (Ref. 31).

The experimental evidence, Pankove relates, shows that with increasing excitation the emission spectrum changes where the low-energy edge maintains the same shape and the high-energy edge becomes more abrupt. This leads to the conclusion that the radiative transition is not a simple localized recombination at an acceptor center.

The model proposed by Pankove to explain this shift is that the emission is due to tunnel-assisted transitions between spatially separated upper and lower states. In Figure 7 is seen the position-dependent energy-level diagram for a band structure perturbed by the heavy doping (Ref. 31:151). As the quasi-Fermi levels move through the upper and lower states, first the most distant sets of states can participate in the recombination with tunneling over a large distance, and then, at higher excitation rates, higher-energy photons (peak emission energy shifts) are emitted with a shorter tunneling range. Finally, at still higher excitation, localized recombination without tunneling will occur.

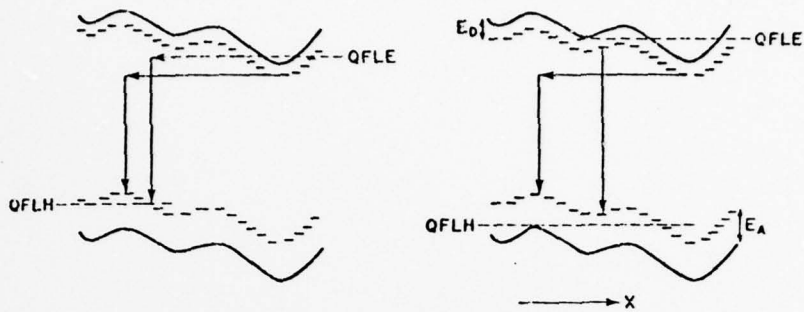


Figure 7. Tunneling-assisted Emission in Compensated GaAs at Low and High Excitation Rates (Ref. 31).

The tunnel-assisted transition model proposed by Pankove might explain peak shifts observed by Walter in carbon implanted GaAs since his samples were heavily compensated with Cr. Since Walter did not consider the key fact of the heavy or close compensation by both the carbon and Cr impurities, he attributed the peak energy shifts strictly to the impurity banding of the carbon impurity. It is, therefore, felt that a more correct interpretation of those results can be given by the tunnel-assisted transition model proposed by Pankove. This subject will be briefly discussed again in light of the results of this thesis in the Results and Discussion chapter.

#### Cathodoluminescence Model

The objective of Cone's research (Ref. 17) was to develop and verify a model describing cathodoluminescence in ion-implanted GaAs. Although his research is not yet completed, the model he developed is complete enough to allow some experimental verification by data

collected on carbon implanted GaAs. The ultimate aim of his research is to predict the luminescence for a specific ion implanted impurity profile in GaAs, as a function of electron beam voltage or as a function of probing depth. A brief discussion of this model, in which some key points of the model are highlighted, will now follow.

The first step taken by Cone was to modify previous work, which had been done on cathodoluminescence for phosphors, to the problem of cathodoluminescence from a uniformly doped semiconductor. The work was next extended to apply to different doping profiles. The profiles of particular interest were to be those that arise from ion-implantation. The problem to be solved was, first, to determine the number of excess minority carriers generated in GaAs by a generating or excitation function which is the energetic electron beam of the cathodoluminescence system used in this thesis and described in the next chapter. Next, the problem was to determine how the excess carriers would recombine at impurity sites (band-to-impurity recombinations), taking into account the fact that an ion-implanted impurity, with an LSS Gaussian density profile, is present in the GaAs. Lastly, the problem was to determine how the relative luminescence intensity, due to excess carriers recombining at ion-implanted impurity sites, would vary as a function of probe energy or the kinetic energy of the energetic electrons in the electron beam. A brief description now follows which highlights Cone's method of solving this problem.

Allowing for the appropriate radiative recombination processes occurring in the crystal, the continuity equation for p-type GaAs minority carriers, created by the electron beam, in one dimension with steady state excitation is given by

$$D_n \frac{d^2n}{dx^2} - \frac{n}{t_n} + g(x) = 0$$

where  $n$  is the excess minority carrier concentration;  $D_n$  is the diffusion constant for GaAs;  $t_n$  is the recombination lifetime of an electron-hole pair in GaAs; and  $g(x)$  is the electron beam excitation function derived from a Monte Carlo analysis similar to work done by Berger (Ref. 32:135-215) and Shimizu et al. (Ref. 33). The Monte Carlo analysis statistically predicts the energy loss of the excitation electrons as they penetrate the GaAs crystal. What is actually calculated are the depth-dose curves for the electrons or the change in energy as a function of penetration depth into the crystal which are similar to, but an improvement of, depth-dose curves arrived at by different means by Norris et al. (Ref. 8) and Wang (Ref. 9). The number of electron-hole pairs generated will then be proportional to the depth-dose curves.

One next assumed that the recombination rate,  $R_n$ , of electron-hole pairs would be

$$R_n = B N(x) n(x)$$

where  $N(x)$  is the density of neutral acceptors predicted by LSS theory;  $n(x)$  is the solution of the continuity equation and has an explicit dependence on  $g(x)$ , the excitation function; and lastly,  $B$  is a proportionality constant. It should be noted that for further

details on values of all the constants used in attaining the solution are described at length in Cone's work. To provide any discussion of those constants was felt to be beyond the scope of this work.

To obtain the cathodoluminescent emission, Cone then integrated over the depth of excitation of the crystal, the rate of radiative recombination. Assuming an exponential absorption of the recombination radiation,  $L(V)$  or the cathodoluminescent emission, is

$$L(V) = \int_0^d B N(x) n(x) e^{-ax} dx$$

where  $B$  is the proportionality constant,  $d$  is an arbitrary cutoff depth,  $N(x)$  is the LSS impurity profile,  $n(x)$  is the excess carrier density, and "a" is the absorption coefficient for the recombination radiation. Since it is only necessary to evaluate  $L(V)$  to within a multiplicative constant, the value of  $B$  does not enter the calculation as long as it is a constant.

In order to normalize the  $L(V)$  curves so that comparisons could be made between different implants, the  $L(V)$  curves were divided by the  $L(V)$  values of a uniformly distributed impurity thought to be present in all GaAs crystals as a result of contamination during the growth phase or annealing phase of the crystal. The impurity contaminant selected was copper because experimental data and a literature search indicated its presence in many cases. However, as the earlier discussion in this section indicated, there is wide disagreement about the correct identification of the 1.35 - 1.37 eV emission band and this ambivalence leads me to believe that the selection of this copper line and its  $L(V)$



curve as a normalizing factor is questionable. This subject will be discussed again briefly in the Results and Discussion section where more evidence is proposed to show why the copper line might not be a proper choice for the normalization.

Although the selection of the copper line might be questionable, certain results of this cathodoluminescence model are noteworthy. The depth-dose curves, for the energetic electrons, as developed for this model provide a good prediction of how the electrons lose their energy as they penetrate the substrate. Some depth-dose curves for the energetic electrons at different energies are shown in Figure 8. In his work, Cone indicates they are in close agreement with the literature and may represent an improvement over other methods of calculating depth-dose curves.

The next illustration is Figure 9 which shows a typical predicted L(V) curve for a carbon-ion implant of  $10^{13}$  ions/cm<sup>2</sup> fluence into a GaAs crystal. The figure indicates that the relative cathodoluminescent intensity curve (upper curve) for the carbon implant has a maximum at an electron beam energy of 8 KeV. The maximum also indicates that, for a beam energy of 8 KeV and the LSS carbon impurity profile, there is no optimal generation of electron-hole pairs in the vicinity of the maximum of the LSS profile curve shown in Figure 1 and of the depth between the maxima of the 5 KeV and 10 KeV depth-dose curves shown in Figure 8.

Although the selection of the uniformly distributed copper impurity is in question, an attempt was made to calculate an L(V) curve for one of the carbon implanted GaAs samples to see how it would compare with

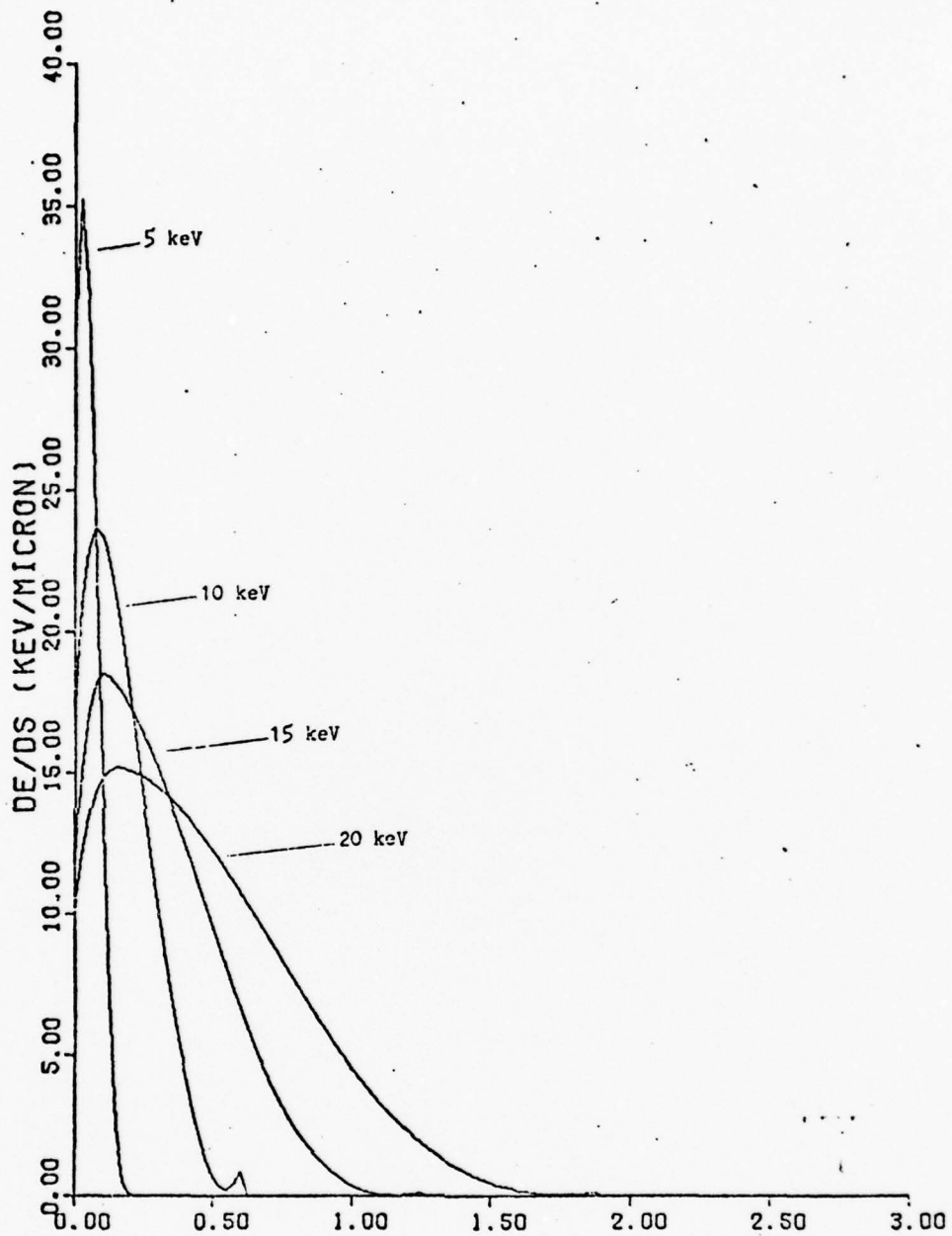


Figure 8. Smoothed Energy Loss Curves for Electrons Incident on GaAs at 45°. Beam energy is noted. Turn up of tail of the 10 KeV Curve is an anomaly of the curve fit routine. (Ref. 17)

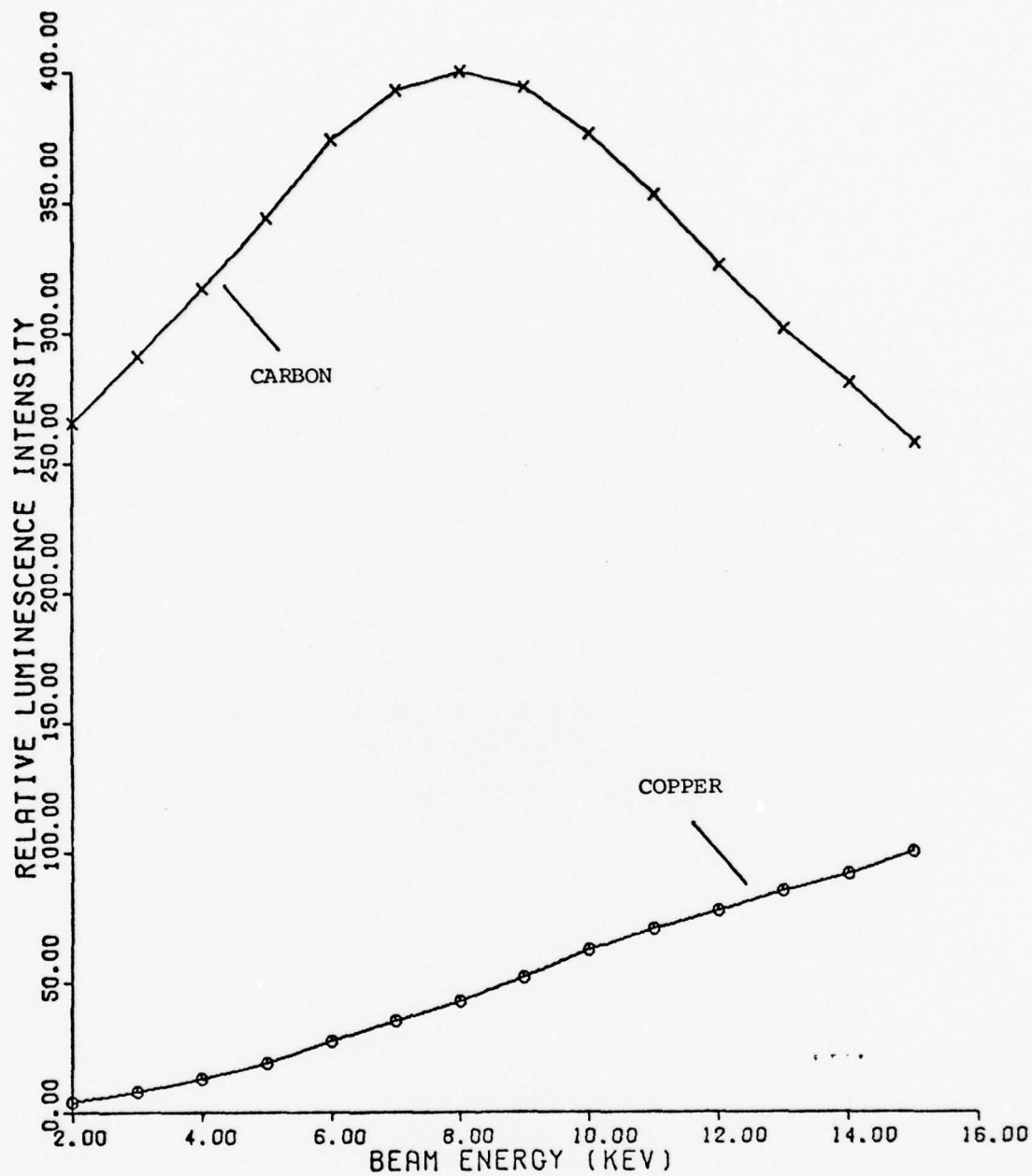


Figure 9. Theoretical L(V) Curve (Upper) for Carbon Ion Implant of  $10^{13}$  ions/cm<sup>2</sup>, at Implant Energy of 120 KeV, Into GaAs. The lower curve is a calculated L(V) curve for the assumed, uniformly distributed, impurity copper. (Ref. 17)

the predicted curve. It was assumed that the 1.36 eV luminescent peak was copper and it was used to normalize the band-impurity luminescent peak at 1.494 eV, which is identified as the band to carbon acceptor transition. Results of this comparison and the details are shown and discussed in the Results and Discussion section.

### III. Results and Discussion

Before the results are discussed, a brief description of the cathodoluminescence system and how the data were obtained is provided. The present system evolved from a very similar system used by Cone (Ref. 17), Walter (Ref. 14) and Dumoulin (Ref. 12), where Dumoulin's is somewhat less similar. A diagram of the cathodoluminescence system is shown in Figure 10.

The electron gun, manufactured by Hughes Aircraft Company and locally modified, provides the electron beam for sample excitation. The vacuum is maintained by two diffusion pumps with a common mechanical forepump. Sample mounting and cooling, luminescence detection and the signal processing are described in detail in Walter's work and only a few key details are now discussed. The cathodoluminescence was analyzed with a Spex 1702 Czerny-Turner spectrometer and detected with an RCA C70007A photo-multiplier tube cooled to  $-50^{\circ}$  C. The photo-multiplier converts incident photons into pulses which are then amplified, in stages, and input into a Multi-Channel Analyzer or MCA. The MCA counts these pulses into channels which are advanced at a preselected rate with respect to the scanning rate of the spectrometer. The relative luminescent intensity, whenever mentioned in this work, refers to these counts which the MCA stores into the channels.

The experimental results of this thesis are discussed in the same sequence as appeared in the Theory and Previous Work section of this thesis. The transitions responsible for the observed luminescent peaks will be discussed in light of the experimental results and the

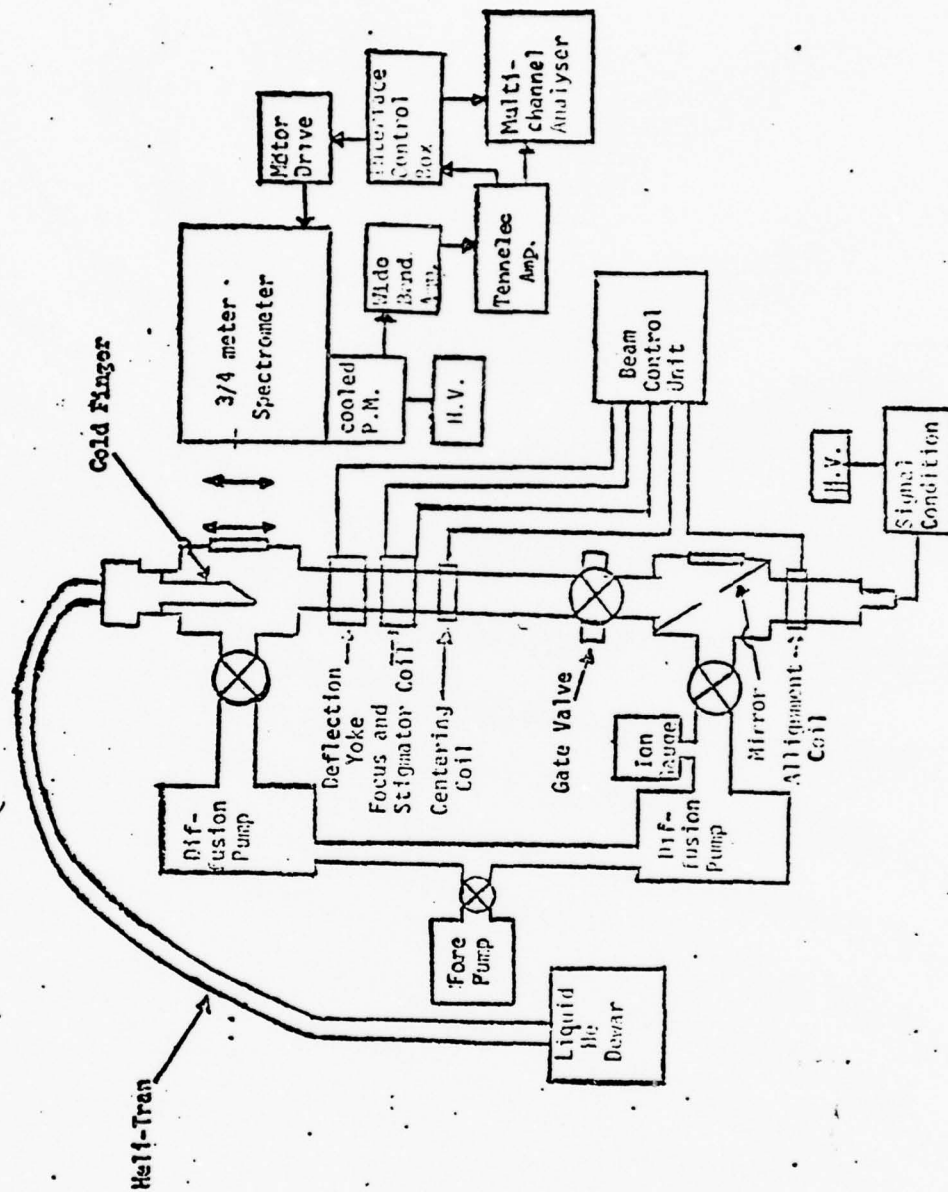


Figure 10. Cathodoluminescence System Diagram (Ref. 14)

literature. Next, the results of attempts to observe luminescence peak energy shifts will be presented. Finally, the results of the relative luminescent intensity or  $L(V)$  curve is calculated from the data and compared to the results of the cathodoluminescence model for GaAs developed by Cone.

All peak energies have been calculated from the raw channel number data of the MCA and all relative intensities are also based on raw channel number photon counts of the MCA with the intensity ratios, whenever discussed, being the ratios of these MCA counts. In the majority of cases, data were recorded at a rate of approximately 1.74 angstroms per channel. This translates to peak energies being accurate to, at best,  $\pm 1$  MeV .

Table I, which follows, assigns sample numbers and preparation conditions for all the samples which will be discussed. To simplify referencing and comparisons, the original sample numbers as assigned by the respective workers are retained.

#### Luminescence Peak Energies

Typical spectra for samples 34, 36 and 37 taken at  $10^\circ$  K are shown in Figures 11, 12 and 13. The spectra exhibit eight peaks which are consistently observable, under various conditions, and which are, in eV, 1.514 , 1.494 , 1.490 , 1.487 , 1.457 , 1.454 , 1.408 and 1.361 .

The 1.514 eV peak has been observed in other studies and has been identified as unresolved excitons and neutral donor-valence band transitions (Refs. 35:995, 36:333). These references also include the possibility of excitons bound to ionized donors which could be

TABLE I

## Sample Numbering and Preparation Conditions

| Sample No.      | Implant Ion<br>@ 120 keV       | Implant Fluence                   | Substrate             | Cap                            | Annealing  |
|-----------------|--------------------------------|-----------------------------------|-----------------------|--------------------------------|--|
| 1 <sup>a</sup>  | RT C <sup>+</sup><br>@ 120 keV | 10 <sup>13</sup> /cm <sup>2</sup> | SI Cr doped           | Si <sub>3</sub> N <sub>4</sub> | 900°C for 15 min in flowing Ar                         |
| 2 <sup>a</sup>  | RT C <sup>+</sup><br>@ 120 keV | 10 <sup>13</sup> /cm <sup>2</sup> | SI Cr doped           | SiO <sub>2</sub>               | 800°C for 15 min in flowing Ar                         |
| 3 <sup>a</sup>  | RT C <sup>+</sup><br>@ 120 keV | 10 <sup>14</sup> /cm <sup>2</sup> | SI Cr doped           | Si <sub>3</sub> N <sub>4</sub> | 800°C for 15 min in flowing Ar                         |
| 4 <sup>a</sup>  | RT C <sup>+</sup><br>@ 120 keV | 10 <sup>13</sup> /cm <sup>2</sup> | SI Cr doped           | Si <sub>3</sub> N <sub>4</sub> | 800°C for 15 min in flowing Ar                         |
| 26 <sup>b</sup> | RT C <sup>+</sup><br>@ 120 keV | 10 <sup>13</sup> /cm <sup>2</sup> | VPE on<br>SI Cr doped | Si <sub>3</sub> N <sub>4</sub> | 800°C for 15 min in flowing Ar<br>with Ga overpressure |
| 28 <sup>b</sup> | RT C <sup>+</sup><br>@ 120 keV | 10 <sup>13</sup> /cm <sup>2</sup> | VPE on<br>SI Cr doped | SiO <sub>2</sub>               | 800°C for 15 min in flowing Ar<br>with Ga overpressure |
| 34 <sup>c</sup> | RT C <sup>+</sup><br>@ 120 keV | 10 <sup>13</sup> /cm <sup>2</sup> | VPE on<br>SI Cr doped | Si <sub>3</sub> N <sub>4</sub> | 850°C for 15 min in flowing Ar                         |
| 36 <sup>c</sup> | RT C <sup>+</sup><br>@ 120 keV | 10 <sup>14</sup> /cm <sup>2</sup> | VPE on<br>SI Cr doped | Si <sub>3</sub> N <sub>4</sub> | 850°C for 15 min in flowing Ar                         |
| 37 <sup>c</sup> | RT C <sup>+</sup><br>@ 120 keV | 10 <sup>15</sup> /cm <sup>2</sup> | VPE on<br>SI Cr doped | SiO <sub>2</sub>               | 850°C for 15 min in flowing Ar                         |

a. Walter (Ref 14).

b. Physics Dept. Staff.

c. Present work.



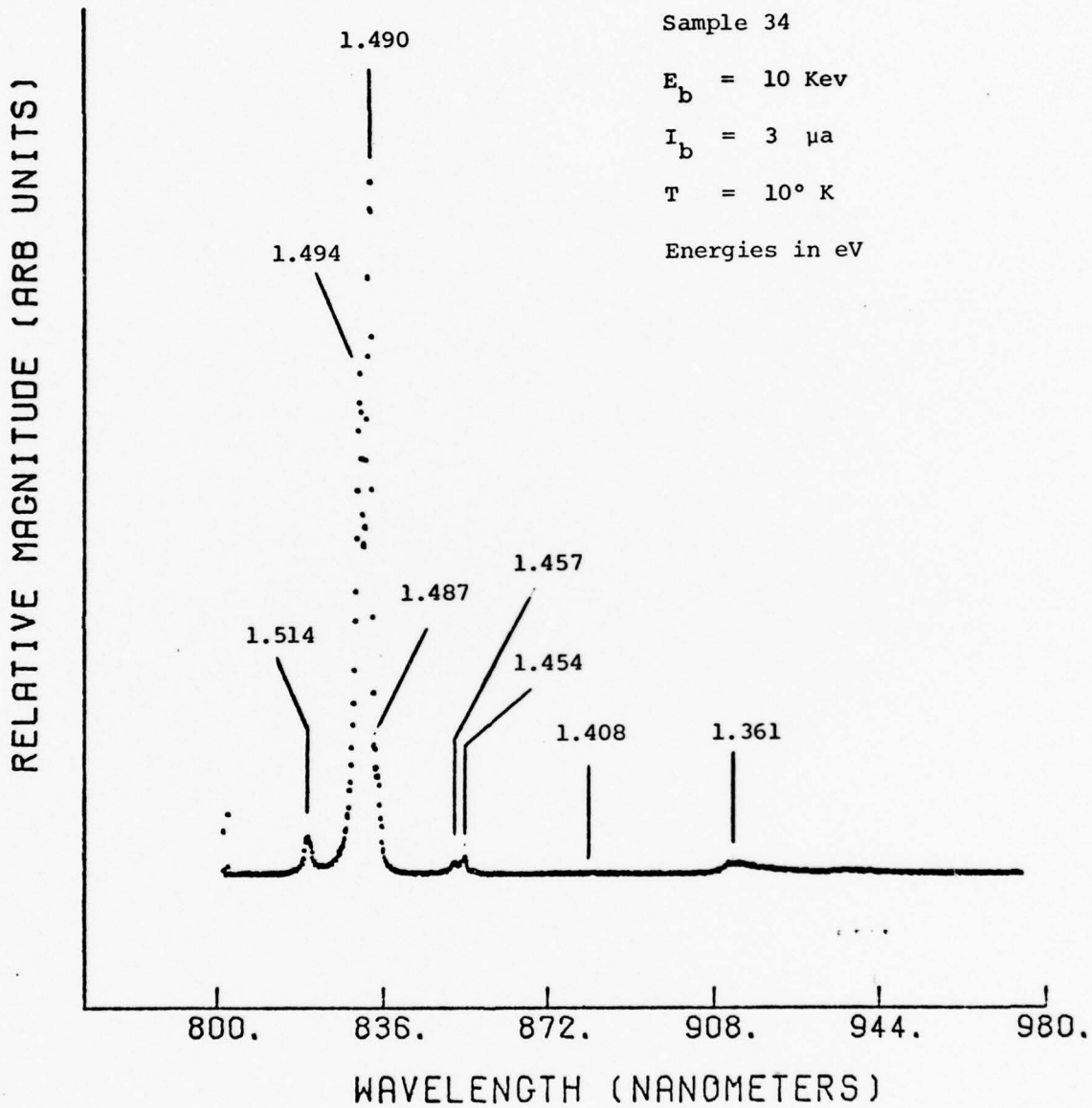


Figure 11. Typical Spectrum for Sample 34

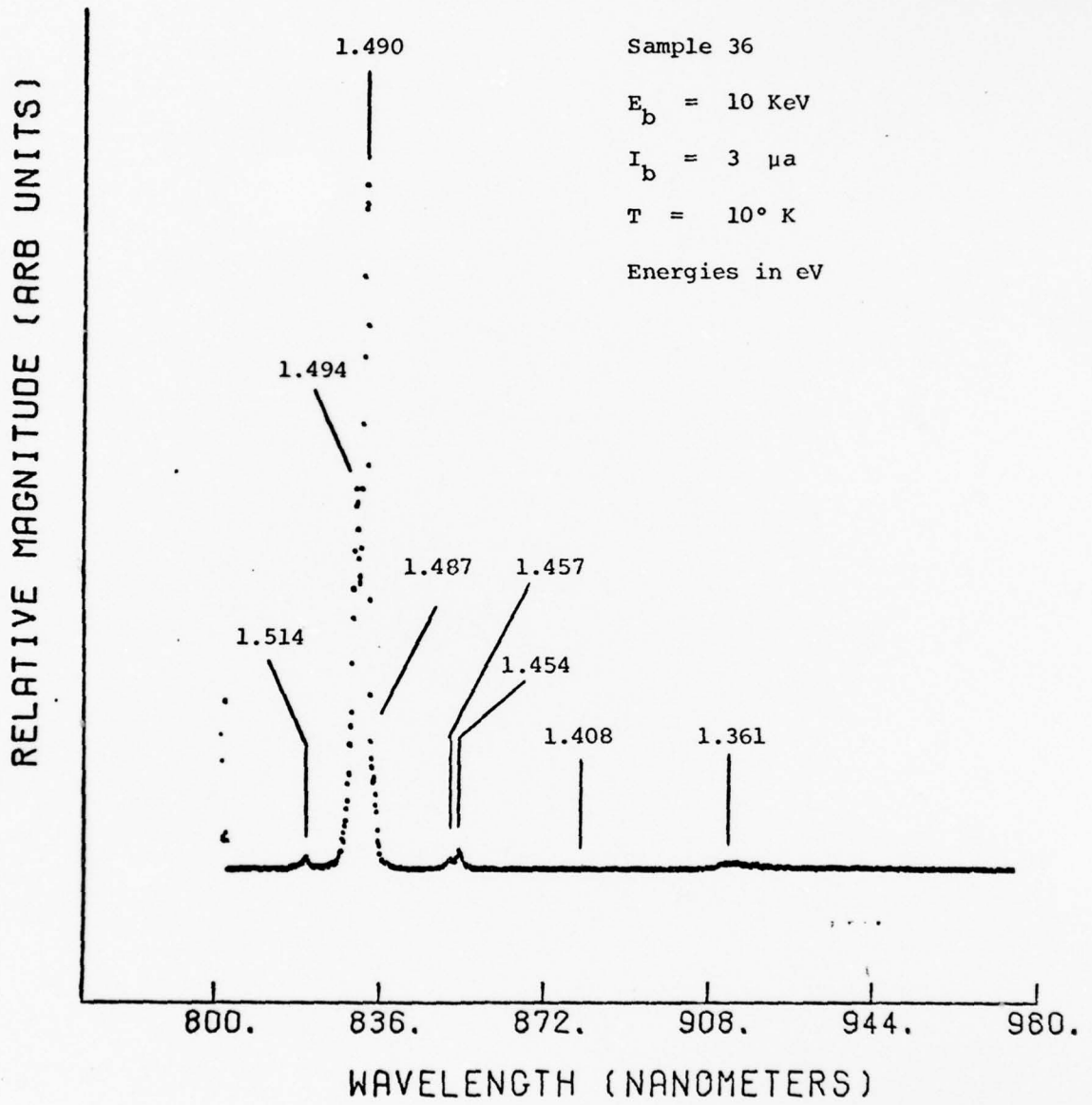


Figure 12. Typical Spectrum for Sample 36

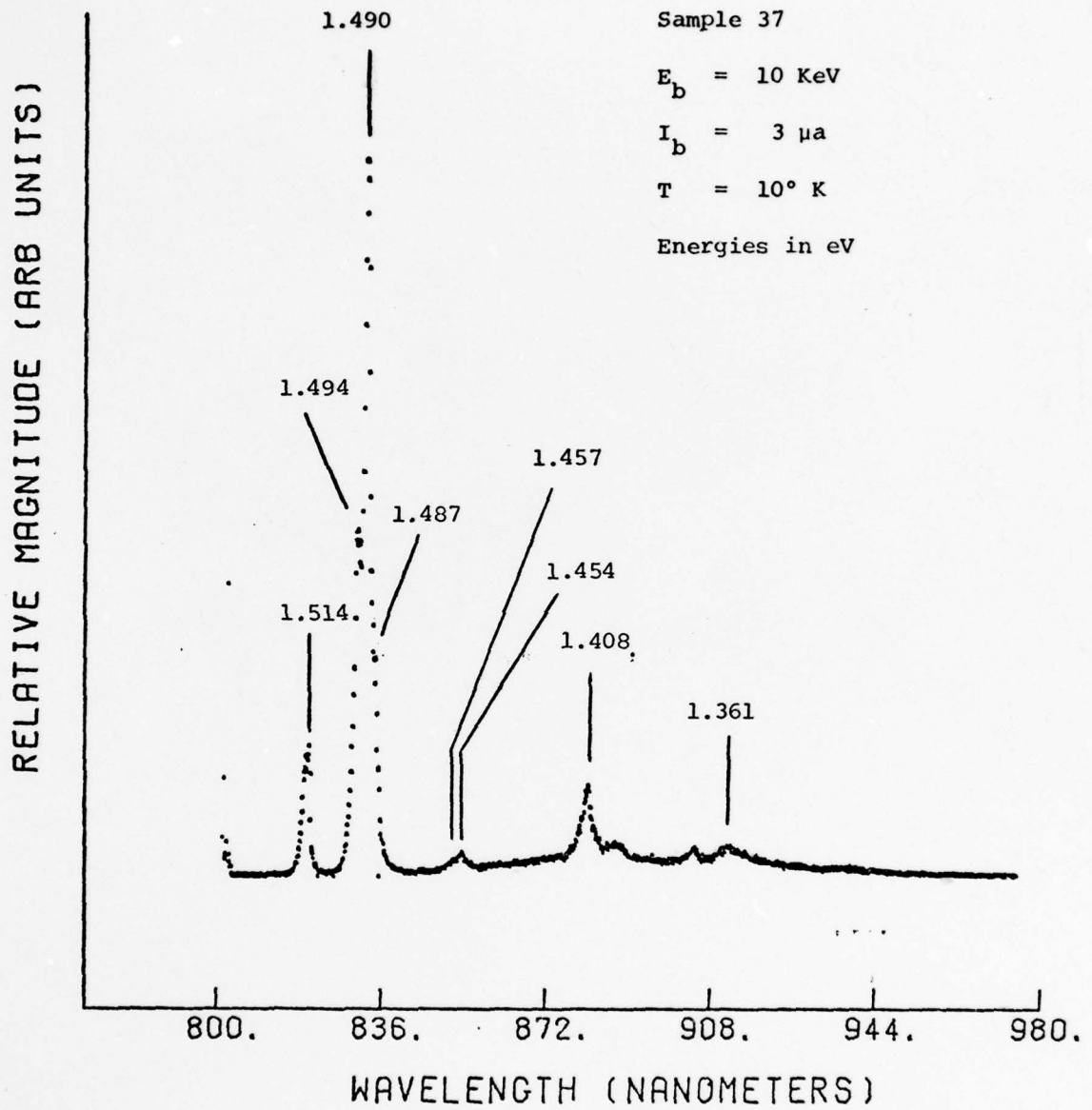


Figure 13. Typical Spectrum for Sample 37

evidenced by noting the rise in relative intensity of this peak when the spectrum for sample 34 taken at approximately 39° K is noted in Figure 14. At this temperature, shallow donors are ionized which allows the formation of these bound excitons and the subsequent annihilation with the emission near 1.514 eV .

The next three peaks, the 1.494 eV , 1.490 eV , and 1.487 eV peaks, are discussed together because they have appeared together in the literature and have posed some problems of interpretation (Refs. 35:996, 37 and 28:349-351). A good example of these three peaks is seen in Figure 15, the spectrum taken from sample 34, where the 1.494 eV and 1.490 eV peaks are clearly resolved and the 1.487 eV peak appears as a shoulder on the low energy side of the 1.490 eV peak.

In an early work, Bogardus and Bebb (Ref. 35) performed temperature dependence studies on n-type and p-type vapor-grown epitaxial GaAs and assigned an observed 1.4936 eV peak to a band-acceptor transition and a 1.4857 eV peak to a donor-acceptor and tentatively assigned a 1.4886 eV peak to an exciton-ionized acceptor complex. They further noted that the broad-band photoluminescence spectra typical of bulk-grown or low-purity epitaxial GaAs breaks into a number of sharp emission lines in very-high-purity GaAs. This could explain why Walter (Ref. 14) observed only a broad band around 1.491 eV , the band-acceptor transition, for his luminescent studies of samples 1, 2, 3 and 4, which are bulk-grown low-purity GaAs. In a subsequent work to that of Bogardus and Bebb, performed by Rossi, et al. (Ref. 37), a magnetic field was utilized in photoluminescence studies with the

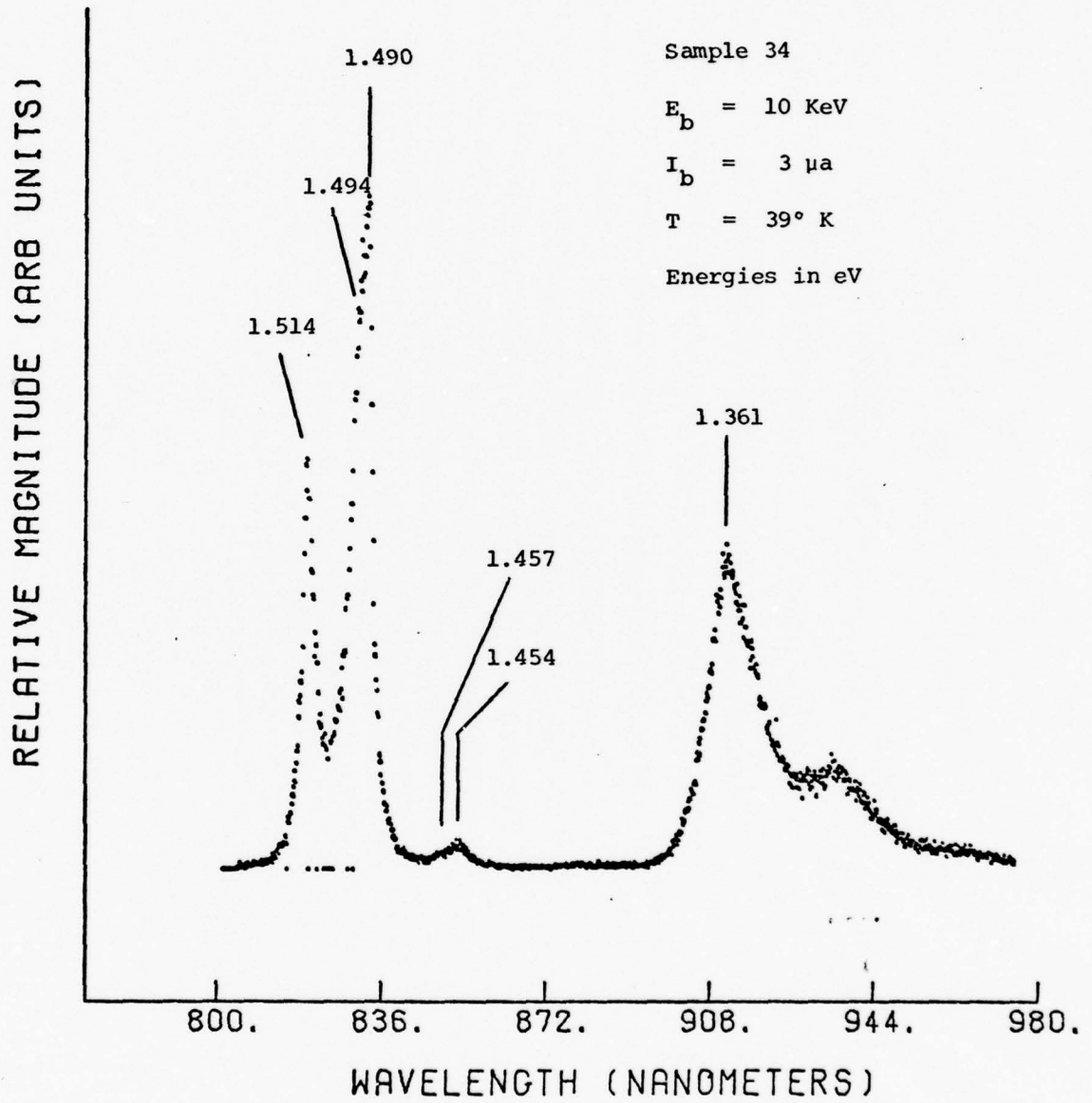


Figure 14. Spectrum of Sample 34 Taken at 39° K

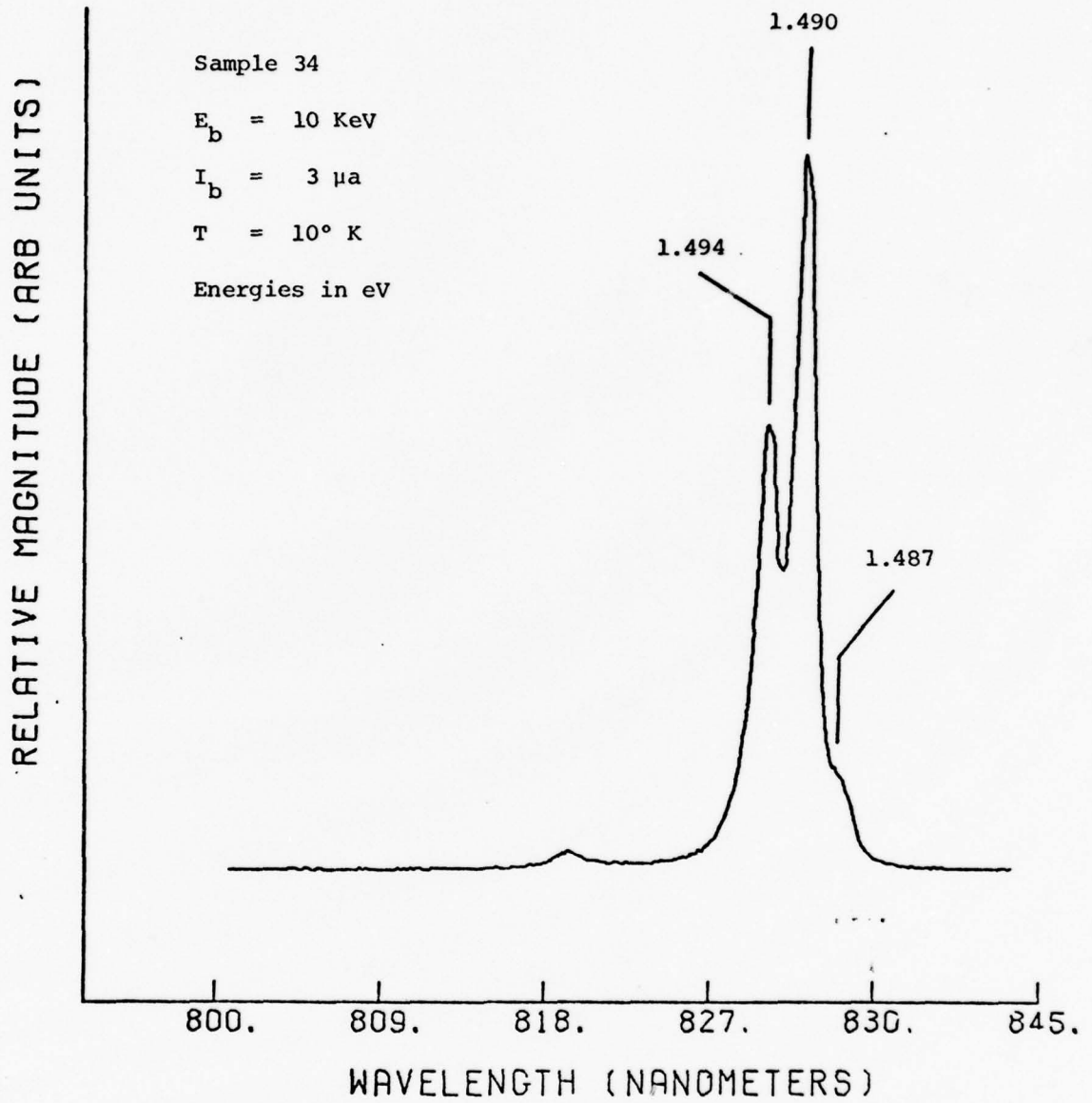


Figure 15. Spectrum of Sample 34 - Three Peaks

result that the 1.4899 eV peak was assigned to a donor-acceptor transition rather than an exciton-ionized acceptor complex, the 1.4861 eV peak remained a donor-acceptor transition, and the 1.4933 eV peak remained a band-acceptor transition. This work was supported by Williams and Bebb (Ref. 28:351) which based their arguments on the fact that, for the exciton-ionized acceptor complex to be stable, theory indicates that the inverse effective mass ratio,  $\sigma^{-1} = m_h/m_e$ , must be less than unity and probably less than about 0.4. Now, since in GaAs  $\sigma^{-1} = 6.67$ , they argued that one would not expect ionized acceptors to bind excitons.

One more study which supports part of this interpretation was done by Kamiya and Wagner (Ref. 38:3222) in which they have observed an emission peak near 1.494 eV which they associate with a band-acceptor transition and one near 1.489 eV which they associate with donor-acceptor transitions. The spectra were photoluminescence spectra of n-GaAs partially compensated with a carbon acceptor.

Considering the above arguments and analyzing the spectra of samples 34, 36 and 37, one notices that the relative intensity ratios of the 1.490 eV peak to the 1.494 eV peak are 1.4, 1.8 and 2.1 for carbon-ion implant fluences of  $10^{13}$ ,  $10^{14}$ , and  $10^{15}$  ions/cm<sup>2</sup>, respectively. Now, since carbon is an amphoteric impurity, it can occupy, substitutionally, both Ga and As sites as an acceptor and a donor, respectively. Hence, one would expect that, as more and more carbon is implanted into the sample, the donor-acceptor transitions should dominate at lower temperatures. If one takes the band gap energy to be 1.521 eV at 10° K, the carbon (acceptor) binding energy,  $E_a$ , to be 26.0 meV (Ref. 39) and the carbon (hydrogenic)

donor) binding energy,  $E_d$ , to be 4.5 meV, we have for the carbon-carbon or donor-acceptor transition a peak energy of

$$E = 1.521 \text{ eV} - E_a - E_d = 1.490 \text{ eV}$$

which is the observed peak energy. Hence, as higher fluences of carbon are implanted into the samples, the carbon-carbon transition peak intensity increases relative to the band-carbon peak intensity. The band-acceptor should not begin to dominate until higher temperatures are reached. This dominance is apparent from Figure 14, the spectrum for sample 34, taken at about 39° K in which the ratio of relative intensities of the 1.490 eV peak to the 1.494 eV peak is now only 1.1 as opposed to 1.4 at 10° K. It should also be noted that the band-carbon transition peak has shifted slightly to 1.493 eV due to the band gap shrinkage at the higher temperature.

The third peak of the trio, 1.487 eV, is considered to be most likely a common residual acceptor contaminant, zinc. For a binding energy of 30.7 meV (Ref. 39) and a hydrogenic donor energy of 4.5 meV, the donor-zinc acceptor transition is approximately 1.486 eV which is too low. Hence, the 1.486 eV peak is most likely due to the donor (possibly carbon)-zinc acceptor transition. Again, this transition dies off and is unresolved at higher temperature as observed in Figure 14, the spectrum for sample 34, taken at about 39° K.

The next two energy peaks at 1.457 eV and 1.454 eV are very close to those expected for the longitudinal optical phonon (LO) emissions coupled to the zero-phonon lines 1.494 eV and 1.490 eV,



respectively. The optical phonon energy separation,  $E_p$ , is taken to be  $36 \text{ meV} \pm 2 \text{ meV}$  (Ref. 40:257) and the observed phonon emissions are in close agreement to this value. It should be noted that in several spectra (not shown) for sample 34, a weak but detectable peak was observed at  $1.450 \text{ eV}$  which is likely the optical phonon coupled to the zero-phonon  $1.487 \text{ eV}$  donor-zinc acceptor emission.

The next two, and last, emission peaks to be discussed are the most controversial because of lack of agreement between previous work done by Walter, and this present study and the literature. They are the broad band energy peaks near  $1.408 \text{ eV}$  and the  $1.361 \text{ eV}$ . These two peaks were discussed at length in the Theory and Previous Work section and the spectra on samples 34, 36 and 37, taken during this study, provide ambiguous results as might have been expected. In his thesis, Walter (Ref. 14:54) studied the effects of  $\text{SiO}_2$  and  $\text{Si}_3\text{N}_4$  caps after annealing and concluded that the  $\text{Si}_3\text{N}_4$  cap allowed greater out-diffusion of As and the  $\text{SiO}_2$  cap allowed greater out-diffusion of Ga during annealing. He also identified a peak emission at  $1.404 \text{ eV}$  which he attributed to the As vacancy-carbon acceptor complex and a peak emission at  $1.359 \text{ eV}$  which he attributed to the band-Ga vacancy complex. His data supported his findings very well and similar findings have been referenced in the Theory and Previous Work section.

The results obtained on samples 34 and 36 are not in agreement with the findings of Walter and others. In fact, for samples 34 and 36, which had  $\text{Si}_3\text{N}_4$  caps, the  $1.408 \text{ eV}$  emission was consistently of low relative intensity and frequently not observable under different

electron beam energies and currents. Typical spectra are shown in Figures 16 and 17 for sample 34 for varying voltages and currents, respectively. They do not show any dominant peaks as Walter observed for his  $\text{Si}_3\text{N}_4$  capped samples. One plausible explanation for this difference is the fact that Walter's samples were bulk-grown SI Cr compensated GaAs which is of lower purity and which certainly had greater densities of native defects such as As vacancies. When these  $\text{Si}_3\text{N}_4$  capped samples were annealed, even more As vacancies were created by As out-diffusion. The VPE GaAs samples, however, are of higher purity with many fewer native defects such as As vacancies and, therefore, annealing of these samples did create As vacancies, but not of the same order as for the bulk-grown samples. The end result is a very low relative intensity of the 1.408 eV As vacancy-carbon acceptor transition observed in Figures 16 and 17.

These results become even more conflicting when the spectra for sample 37 ( $\text{SiO}_2$  capped) are noted in Figure 18 for varying beam voltages. The effect of the  $\text{SiO}_2$  cap, which should have allowed out-diffusion of Ga, on sample 37 is not evident from the spectra. There is a fairly sharp peak at 1.408 eV, the peak attributed to As vacancy complexes, and the 1.361 eV peak, attributed by some to a Ga vacancy complex, is not prominent which is again contrary to Walter's results. A possible explanation is that excessive implant damage, not recorded by annealing, remained as residual defects with emission energy peaks near 1.40 eV.

The results from cathodoluminescence studies of samples 26 and 28 also do not aid in the resolution of this problem with the 1.408 eV and 1.361 eV peaks. As can be seen in Table I, sample 26 was capped

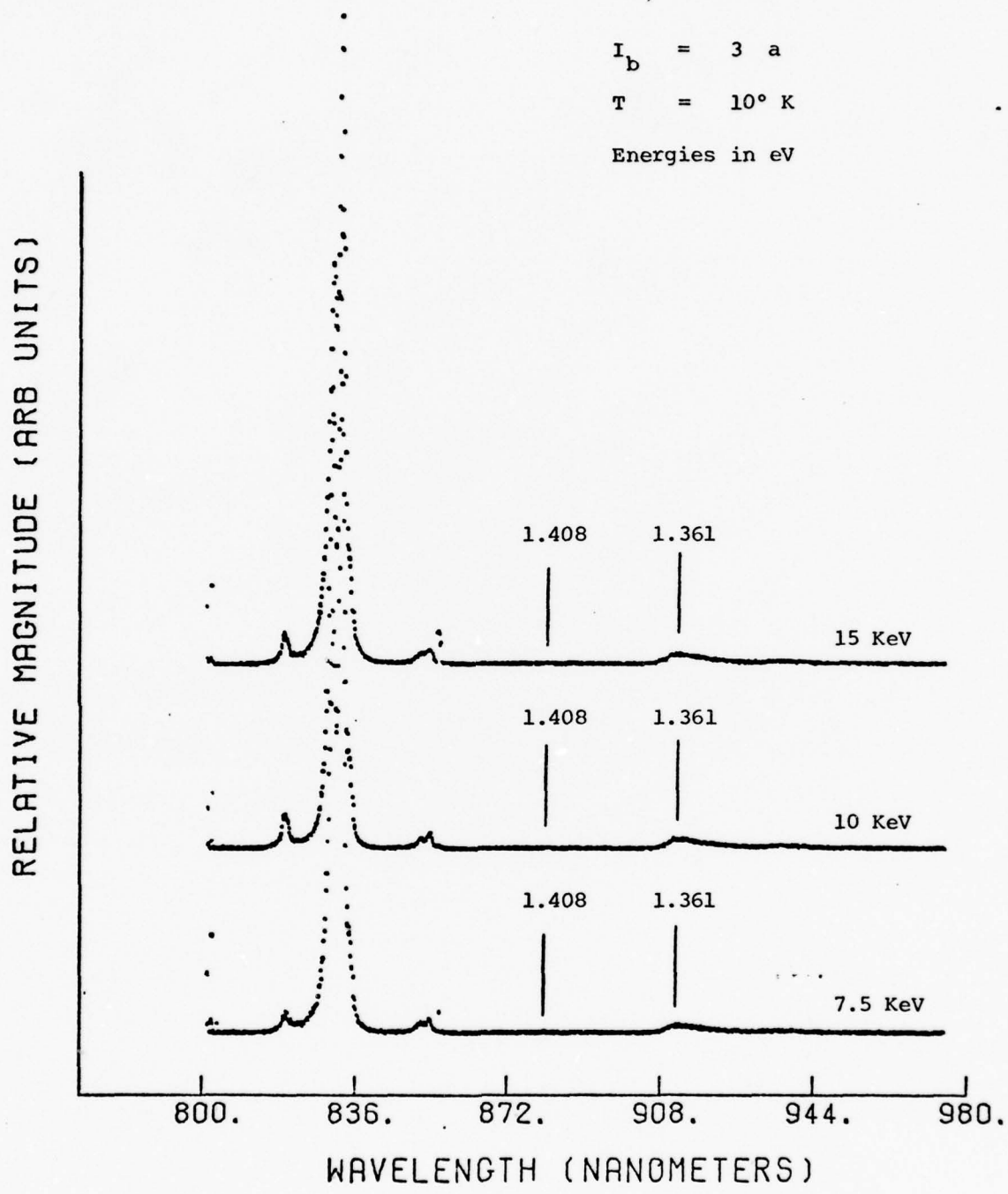


Figure 16. Spectra for Sample 34 at Different Beam Voltages

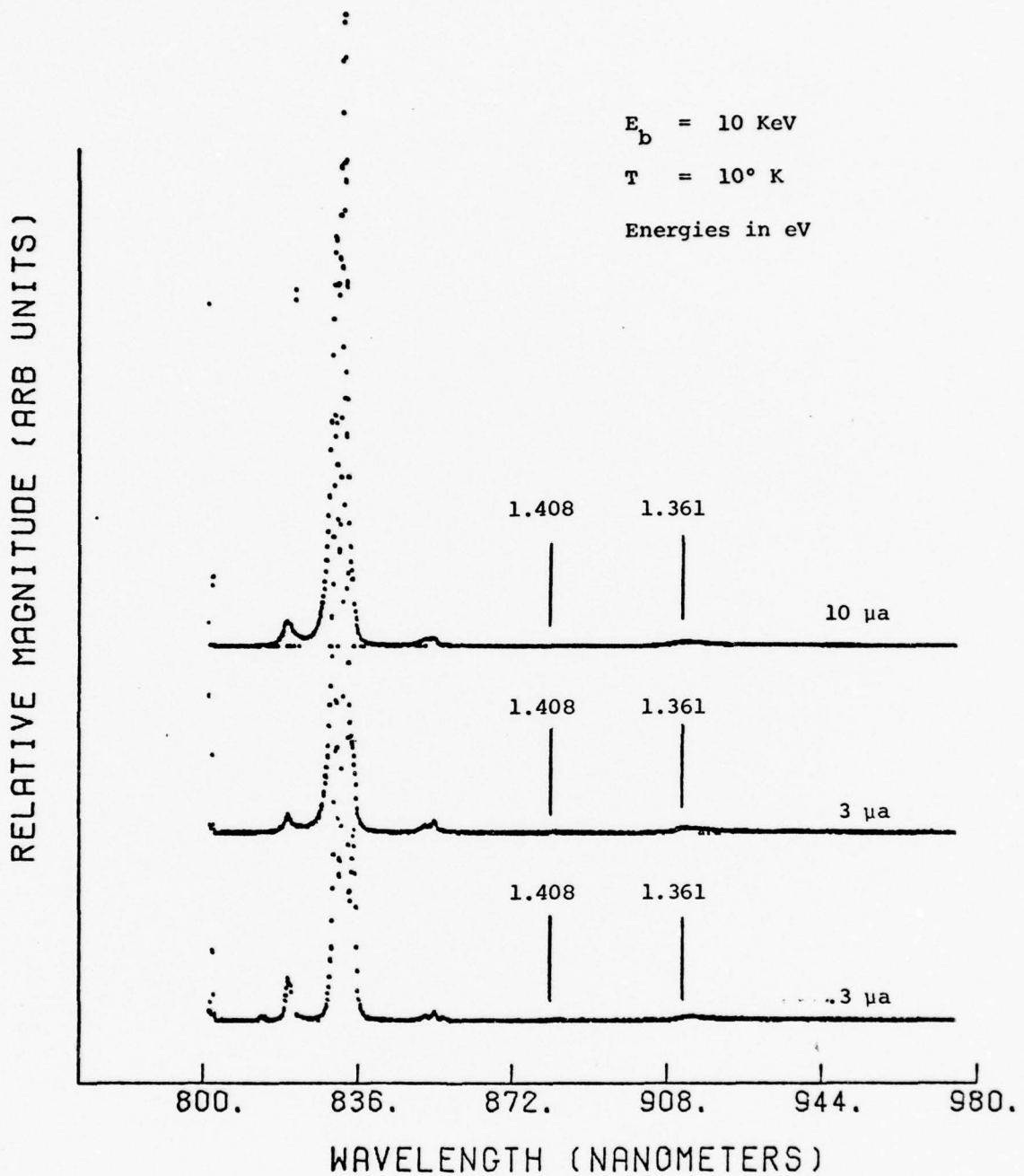


Figure 17. Spectra for Sample 34 at Different Beam Currents

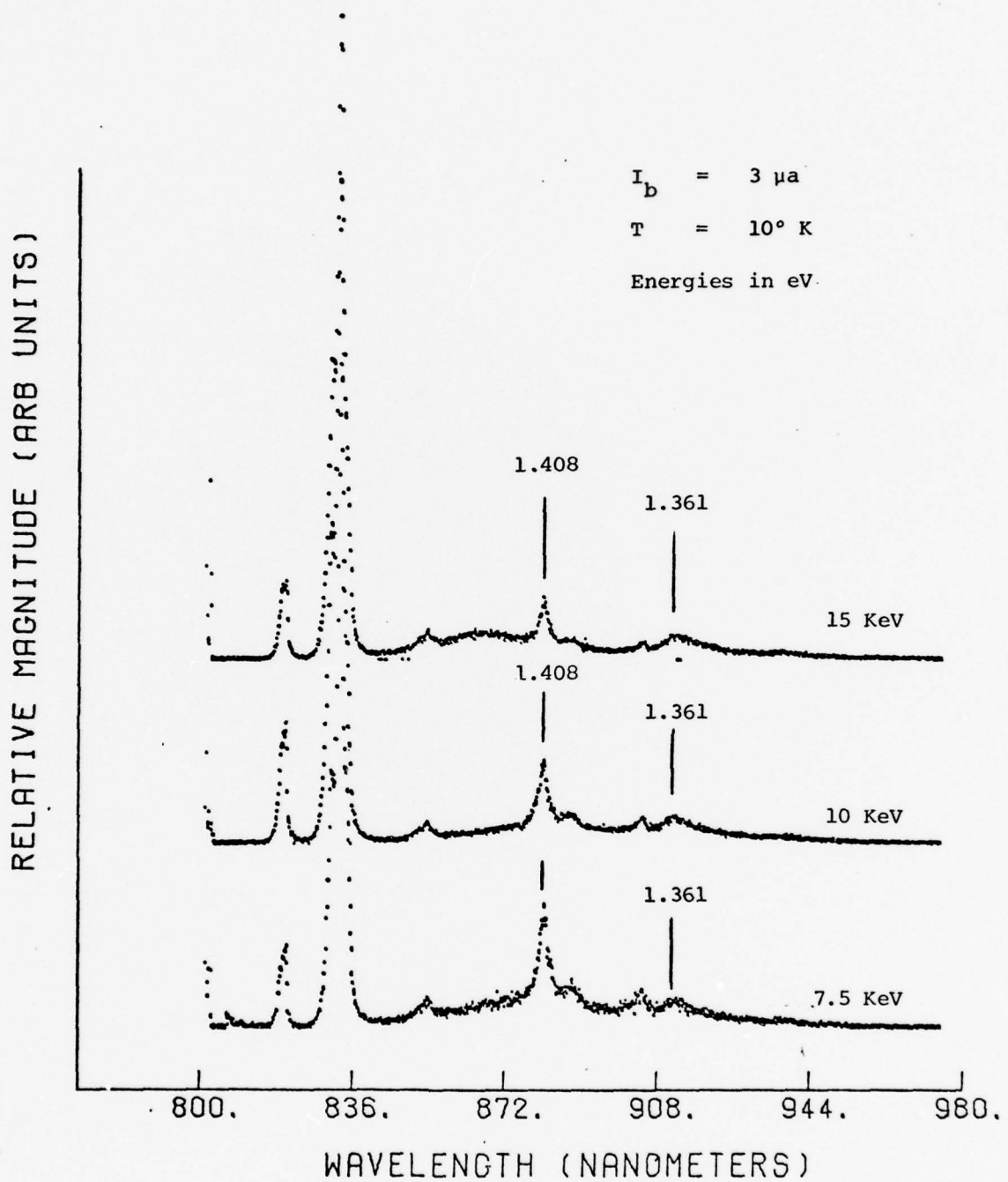


Figure 18. Spectra for Sample 37 at Different Beam Voltages

with  $\text{SiO}_2$  and annealed like all other samples, except that these two samples also had an overpressure of Ga during annealing. The interesting result is that neither the 1.408 eV or the 1.361 eV peaks are observable at any electron beam voltage (2.5 - 15 KeV) or current. This returns us to the maxim stated earlier -- annealing studies always tend to indicate that vacancies are the cause for observed emission peaks. That is, the results for samples 26 and 28 indicate that Ga vacancies were responsible for the 1.361 eV peak (possibly copper on Ga sites also) and may also have an effect on the 1.408 eV peak since Ga vacancies and As vacancies seem to have a mutual effect on each other. Again, the results are apparently not conclusive. Although the 1.361 eV peak was discussed at length in the Theory section and was identified by Walter as a band-acceptor (Ga vacancy), its identity remains in question because of the variance in the results of this work with those of previous work. It seems logical to assume that the true identity strongly depends upon the GaAs crystal growth and annealing history with the identity being one for certain conditions and another for different conditions.

#### Peak Energy Shifts

No luminescence peak energy shifts were observed for the epitaxial GaAs samples. In an attempt to repeat Walter's observations, which were discussed in the Theory and Previous Work section, cathodoluminescence spectra from selected samples of VPE GaAs crystals grown on SI Cr compensated GaAs substrate were analyzed (see samples 26, 28, 34, 36 and 37, Table I). The absence of peak energy shifts for the VPE GaAs is in agreement with the findings of Pankove, for n- or p-type GaAs of

moderate or heavy doping, which have been discussed in the Theory and Previous Work section of this thesis. Depth-profiling of the samples mentioned above failed to show any depth or impurity concentration dependent peak energy shifts for carbon ion implant doses or fluences of  $10^{13}$  ,  $10^{14}$  , and  $10^{15}$  ions/cm<sup>2</sup> . The main difference between these samples and Walter's samples is the fact that Walter's samples were SI Cr compensated GaAs substrate, whereas the samples analyzed for this thesis were high-purity VPE GaAs layers grown on SI Cr compensated GaAs substrates. The VPE layers had only the carbon ion implanted impurity, whereas Walter's samples were heavily compensated with approximately  $10^{16}$  -  $10^{17}$  Cr atoms/cm<sup>3</sup> and then ion implanted with carbon at fluences of  $10^{13}$  ,  $10^{14}$  and  $10^{15}$  ions/cm<sup>2</sup> (approximately  $10^{16}$  -  $10^{17}$  carbon ions/cm<sup>3</sup> ) . It would seem then that Walter's samples could be described as closely compensated and that Walter's observations of peak energy shifts could be explained by Pankove's tunnel-assisted transitions in closely compensated GaAs. Hence, what Walter observed may have been the combined effects of both the carbon impurity and the Cr impurity. Since the VPE GaAs samples studied during this thesis did not contain significant amounts of Cr impurities, the peak energy shifts were not observed, it is surmised, for this reason. The effects of band tailing and compensation have been widely studied (Refs. 4, 5, 29, 30, 31:107-152, as a selected few) and can account, at least qualitatively, for energy shifts as reported by Walter. Unfortunately, any quantitative analysis of compensation would require electrical measurements of the samples and the data were not available for the samples in question.

Although an attempt was made to detect excitation dependent peak energy shifts (as evidence of banding or band tails), the cathodoluminescence system could not provide a wide enough range of excitation to create noticeable peak energy shifts due to donor-acceptor recombinations and near/far pair considerations discussed earlier in the Theory section. A good method for determining whether shifts are occurring due to donor-acceptor transitions in heavily doped materials is time-resolved cathodoluminescence, also briefly described by Pankove in terms of photoluminescence. This would be an excellent area for further study since the required equipment is available.

#### Cathodoluminescence Model

In order to apply data obtained during this work to the cathodoluminescence model developed by Cone, at least two assumptions must first be made: first, the 1.361 eV energy peak is assumed to be due to copper (on Ga sites), a uniformly distributed impurity, since that was the assumption made by Cone; and, second, the relative luminescent intensities of both the 1.494 eV peak and the 1.361 eV peak can be closely approximated by the photon counts provided by the MCA, rather than calculating the integrated luminescence intensities of each transition, since the luminescence curves for each transition are assumed to be Gaussian in shape. With that proviso, sample 34 was chosen to provide the data since it had the  $10^{13}$  ions/cm<sup>2</sup> carbon implant. The photon counts for each band peak at varying electron beam energy were then tabulated. The band-carbon intensities were divided by the respective copper peak intensities and the results were normalized to the relative intensity,  $L(V)$ , axis of the computer generated



L(V) graph from Cone's model. The result is shown in Figure 19. The L(V) curve generated from the data maximizes at a lower electron beam energy than that predicted by the model and the curve's overall shape on the high energy side deviates from the predicted curve. These deviations could be due to several reasons which are now discussed. The first reason is probably the questionable selection of the 1.361 eV "copper" peak since its identity is in doubt. The second reason is the few data points used since a larger number of points would have to be used for an unbiased comparison. The last reason is the possible incorrect selection of the values for numerous constants that play important roles in this theoretical model, amongst them being diffusion constants, recombination lifetime, diffusion length, and surface recombination velocity, just to name a few. Furthermore, as a start, this model assumes the diffusion length and diffusion constant, for GaAs, are constant in the solving of the continuity equation. This could be inducing error into the model, since the results of other studies indicate that these constants have some depth dependence related to the impurity profile in the crystal. Cone has not finished his work and is still making improvements in different areas of his model.

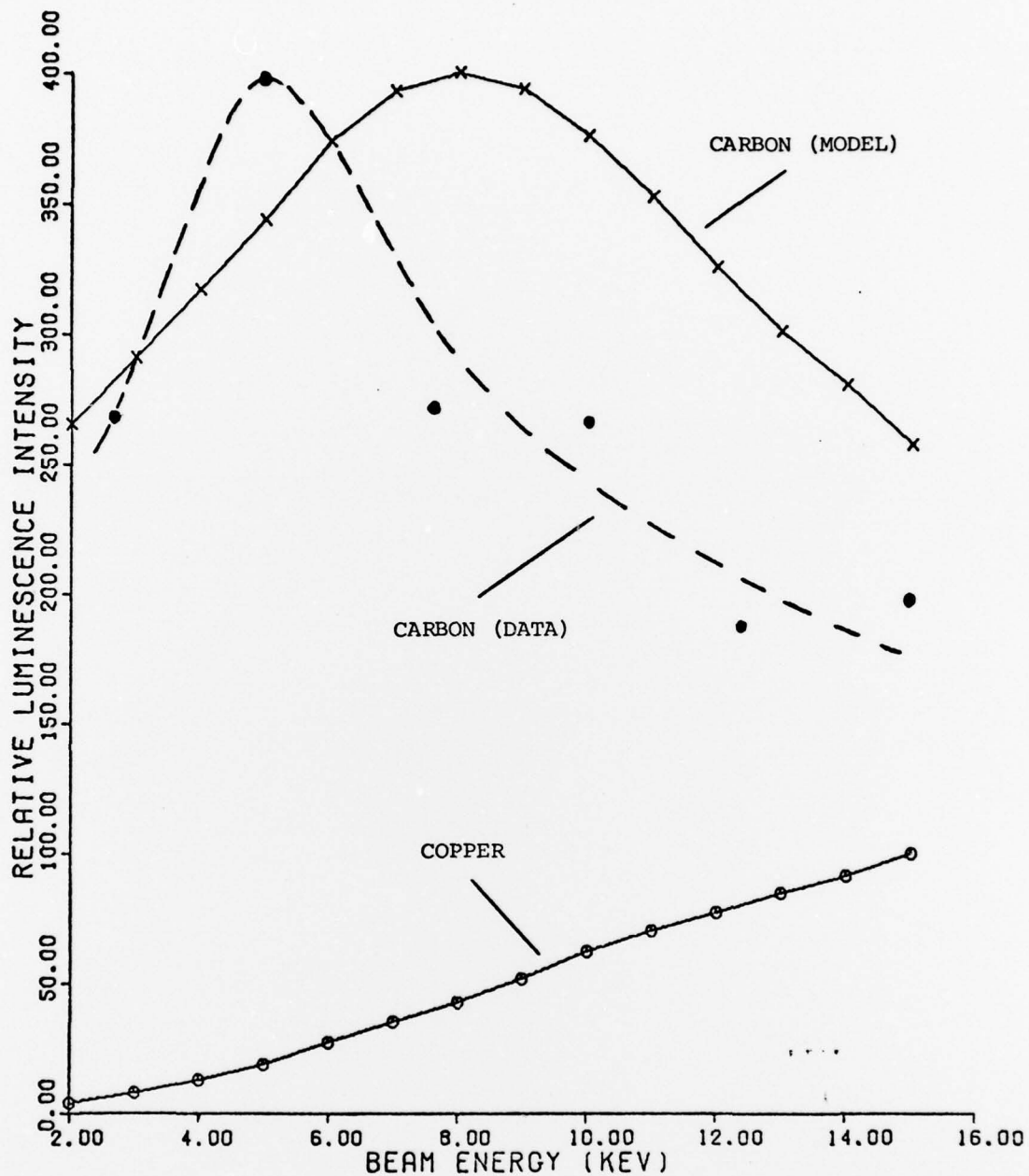


Figure 19. Theoretical L(V) Curve (Solid Upper) Vs. Experimental L(V) Curve (Dashed), for Carbon-Ion Implant of  $10^{13}$  ions/cm<sup>2</sup> at Implant Energy of 120 KeV into GaAs. Lower solid curve is the L(V) curve for copper.

#### IV. Conclusions and Recommendations

##### Conclusions

The spectra obtained from samples 34, 36 and 37 exhibit eight peaks which were consistently observable, under various conditions, and which are: a 1.514 eV peak attributed to unresolved excitons and neutral donor-valence band transitions; a 1.494 eV peak attributed to conduction band-carbon acceptor transitions; a 1.490 eV peak as the carbon donor-carbon acceptor transitions; a 1.487 eV peak as a possible carbon acceptor-zinc donor transition; two phonon peaks at 1.457 eV and 1.454 eV coupled to the zero-phonon peaks at 1.494 eV and 1.490 eV, respectively; a 1.408 eV peak attributed to As vacancy complexes; and, finally, a 1.361 eV peak attributed to either copper on Ga in a vacancy complex or the more elaborate  $\text{As}^+ \text{Cu}^- \text{As}^+$  complex.

Impurity concentration dependent energy peak shifts are not observable in high-purity VPE GaAs crystals which have been carbon-ion implanted with fluences of  $10^{13}$ ,  $10^{14}$  and  $10^{15}$  ions/cm<sup>2</sup>. Although impurity banding has been reported as the cause of energy peak shifts in bulk-grown SI Cr compensated GaAs, the results obtained here support the interpretation that the carbon impurity plus the Cr compensating impurity produced the observed energy peak shifts according to the tunnel-assisted transitions model, for closely compensated GaAs, as proposed by Pankove. The absence of energy peak shifts in the high-purity VPE GaAs crystals, which were not Cr compensated, supports this interpretation.

Although attempts were made to detect the presence of tunnel-assisted transitions, negative results were obtained for all the carbon implanted epitaxial GaAs samples. That is, peak energy shift effects were not observed even though depth-profiling was extensively used at varying current densities. Impurity band-tailing or band edge perturbations were certainly present in the samples and it is concluded that excitation dependent peak energy shifts were not observed because the excitation power (the combined effect of electron beam energy and current density) could not be varied over a sufficiently wide range to observe excitation dependent effects.

No consistent conclusions could be drawn about the effects of  $\text{Si}_3\text{N}_4$  and  $\text{SiO}_2$  encapsulants since the results did not agree with previous results. Since the data taken for this work did not have the objective of studying encapsulant effects, this variance with previous work is more an observation than a conclusion.

The cathodoluminescence model, for ion implanted GaAs, developed by Cone requires more comparisons with experimental data before it can be fairly evaluated. However, one weakness it does have is its dependence upon identifying a known uniformly distributed impurity from which a normalization factor is obtained. The question of the identity of the 1.361 eV band is mainly unresolved and, until it is reasonably resolved, this model has a definite weakness since no other uniformly distributed and observable impurity is presently known.

#### Recommendations

If possible, the cathodoluminescence system should have its power capabilities increased so that some excitation dependent effects

such as donor-acceptor recombination in heavily doped materials could be observed. Perhaps some of the samples already studied could be observed at higher intensity of excitation power. It is felt that this would be a good method for determining whether impurity banding or tunnel-assisted transitions occur in the samples discussed. This would also be a good method of determining whether the 1.490 eV energy peak was, in fact, a donor-acceptor transition.

The other avenue recommended for studying ion implanted GaAs is time-resolved cathodoluminescence. Combining the results of both depth-resolved and time-resolved cathodoluminescence would provide a powerful characterization technique for studying carbon or any other ion implanted into GaAs.

### Bibliography

1. Gergely, G.Y. "Surface Recombination and Diffusion Processes in Cathodoluminescence and Electron Bombardment Induced Conductivity," Journal of Physics and Chemistry of Solids, 17: 112-116 (1960).
2. Cusano, D.A. "Radiative Recombination from GaAs Directly Excited by Electron Beams," Solid State Communications, 2: 353-358 (1964).
3. Wittry, D.B. and D.F. Kyser. "Cathodoluminescence at p-n Junctions in GaAs," Journal of Applied Physics, 36: 1387-1389 (April 1965).
4. Pankove, J.I. "Cathodoluminescence of p-Type GaAs," Proceedings of the International Conference of the Physics of Semiconductors, 298-301, Kyoto, Japan, 1966.
5. -----."Cathodoluminescence of n-Type GaAs," Journal of Applied Physics, 39: 5368-5371 (November 1968).
6. Kurbatov, L.N. "Cathodoluminescence of Gallium Arsenide," Soviet Physics-Semiconductors, 4: 47-51 (July 1970).
7. Woodcock, J.M., et al. "Electrical and Cathodoluminescence Measurements on Ion Implanted Donor Layers in GaAs," Solid State Electronics, 18: 267-275 (1975).
8. Norris, C.B., et al. "Depth-Resolved Cathodoluminescence in Undamaged and Ion-Implanted GaAs, ZnS, and CdS," Journal of Applied Physics, 44: 3209-3221 (July 1973).
9. Martinelli, R.U. and C.C. Wang. "Electron-Beam Penetration in GaAs," Journal of Applied Physics, 44: 3350-3351 (July 1973).
10. Pierce, B.J. Luminescence and Hall Effect of Ion Implanted Layers in ZnO. AFML-TR-75-161. Wright-Patterson AFB, Ohio: Air Force Materials Laboratory (October 1976).
11. Boulet, D.L. Depth-Resolved Cathodoluminescence of Cadmium Implanted Gallium Arsenide, Unpublished Thesis, Wright-Patterson AFB, Ohio: Air Force Institute of Technology (December 1975). (AD A019 950)
12. Dumoulin, J.D. Depth-Resolved Cathodoluminescence on the Effects of Cd Implantation and Annealing in Gallium Arsenide, Unpublished Thesis, Wright-Patterson AFB, Ohio: Air Force Institute of Technology (December 1976). (AD A034 029)
13. Pierce, B.J. and R.L. Hengehold. "Depth-Resolved Cathodoluminescence of Ion-Implanted Layers in Zinc Oxide," Journal of Applied Physics, 47: 644-651 (February 1976).

14. Walter, M.J. Depth-Resolved Cathodoluminescence of Carbon Implanted Gallium Arsenide, Unpublished Thesis, Wright-Patterson AFB, Ohio: Air Force Institute of Technology (December 1977).
15. McKelvey, J.P. Solid State and Semiconductor Physics, New York: Harper and Row, 1966.
16. Pickar, K.A. "Ion Implantation in Silicon - Physics, Processing and Microelectronic Devices," Applied Solid State Science, Volume 5, edited by Raymond Wolfe. New York and London: Academic Press, 1975.
17. Cone, M.L. Cathodoluminescence Characterization of Ion Implanted GaAs, (tentative title), Unpublished Dissertation, Wright-Patterson AFB, Ohio: Air Force Institute of Technology (1978).
18. Sturge, M.D. "Optical Absorption of Gallium Arsenide Between 0.6 and 2.75 eV," Physical Review, 127: 768-773 (August 1962).
19. Kittel, C. Introduction to Solid State Physics. New York: John Wiley and Sons, 1976.
20. Dean, P.J. "Junction Electroluminescence," Applied Solid State Science, Volume 1, edited by Raymond Wolfe. New York and London: Academic Press, 1969.
21. Lin, M.S. "Photoluminescence and Electrical Measurements on Manganese Ion-Implanted GaAs," Japanese Journal of Applied Physics, 15: 53-56 (January 1976).
22. Llegems, M., et al. "Optical and Electrical Properties of Mn-Doped GaAs Grown by Molecular Beam Epitaxy," Journal of Applied Physics, 46: 3059-3065 (July 1975).
23. Chang, L.L., et al. "Vacancy Association of Defects in Annealed GaAs," Applied Physics Letters, 19: 143-145 (September 1971).
24. Cho, A.Y. and I. Hayashi. "Surface Structures and Photoluminescence of Molecular Beam Epitaxial Films on GaAs," Solid State Electronics, 14: 125-132 (1971).
25. Queisser, H.J. and C.S. Fuller. "Photoluminescence of Cu-Doped Gallium Arsenide," Journal of Applied Physics, 37: 4895-4899 (December 1966).
26. Guislain, H.J., et al. "A Coherent Model for Deep-Level Photoluminescence of Cu-Contaminated n-Type GaAs Single Crystals," Journal of Electronic Materials, 7: 83-108 (1978).
27. Chiang, S.Y. and G.L. Pearson. "Properties of Vacancy Defects in GaAs Single Crystals," Journal of Applied Physics, 46: 2986-2991 (July 1975).

28. Williams, E.W. and H.B. Bebb. "Photoluminescence II: Gallium Arsenide," Semiconductors and Semimetals, Volume 8, edited by R.K. Willardson and A.C. Beer. New York and London: Academic Press, 1972.
29. Alderov, Zh.I., et al. "Radiative Recombination in Epitaxial Compensated Gallium Arsenide," Soviet Physics-Semiconductors, 6: 1718-1725 (April 1973).
30. Casey, Jr., H.C. and F. Stern. "Concentration-Dependent Absorption and Spontaneous Emission of Heavily Doped GaAs," Journal of Applied Physics, 47: 631-643 (February 1976).
31. Pankove, J.I. Optical Processes in Semiconductors, Englewood Cliffs, NJ: Prentice-Hall, Inc., 1971.
32. Berger, M.F. "Monte Carlo Calculation of the Penetration and Diffusion of Fast Charged Particles," Methods in Computational Physics, Volume 1, edited by B. Alder, et al. New York and London: Academic Press, 1963.
33. Shimizu, R., et al. "The Monte Carlo Technique as Applied to the Fundamentals of EPMA and SEM," Journal of Applied Physics, 43: 4233-4249 (October 1972).
34. Gibbons, J.F. "Ion Implantation in Semiconductors - Part I, Range Distribution Theory and Experiments," Proceedings of the IEEE, 56: 295-319 (March 1968).
35. Bogardus, E.H. and H.B. Bebb. "Bound-Exciton, Free-Exciton, Band-Acceptor, Donor-Acceptor, and Auger Recombination in GaAs," Physical Review, 176: 993-1002 (December 1968).
36. Venghaus, H. "Excitation Intensity Dependence of Shallow Donor Bound Exciton Luminescence in n-GaAs," Journal of Luminescence, 16: 331-341 (1978).
37. Rossi, J.A., et al. "Acceptor Luminescence in High-Purity n-Type GaAs," Physical Review Letters, 25: 1614-1617 (December 1970).
38. Kamiya, T. and E. Wagner. "Shallow Acceptor Binding Energy and Lifetime of Donor-Acceptor Pairs in Gallium Arsenide," Journal of Applied Physics, 47: 3219-3223 (July 1976).
39. Ashen, D.J., et al. "The Incorporation and Characterization of Acceptors in Epitaxial GaAs," Journal of Physics and Chemistry of Solids, 36: 1041-1053 (1975).
40. Williams, E.W. "A Photoluminescence Study of Acceptor Centres in Gallium Arsenide," British Journal of Applied Physics, 18: 253-261 (1967).

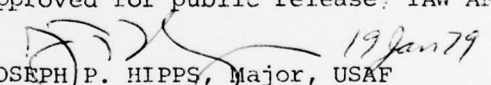


41. Shin, B.K. "Carbon-Ion-Implanted Gallium Arsenide," Applied Physics Letters, 29: 438-440 (October 1976).

### Vita

Luciano Vittorio Parzianello was born on 27 July 1943 in Pozzuolo, Province of Udine, Italy, the son of Olindo and Armida Parzianello. His family immigrated to the United States in 1952 and settled in Dearborn, Michigan where he graduated from high school in 1961. In 1966 he graduated from the University of Michigan with the degree of Bachelor of Science in Physics, and he spent the next year working for the University of Michigan as Research Assistant, Geophysics Laboratory, Willow Run Laboratories. He received a reserve commission in the United States Air Force upon completing Officers Training School in 1968 and then attended the Avionics Maintenance Officer Technical School at Lowry Air Force Base, Colorado. He was then assigned to Clinton-Sherman Air Force Base, Oklahoma. He was reassigned in 1969 to the 319th Bombardment Wing, Grand Forks Air Force Base, North Dakota. In May 1971 he was assigned to U-Tapao Royal Thai Navy Base, Thailand. In January 1973 he was assigned to the 416th Bombardment Wing, Griffiss Air Force Base, New York. His next assignment, in August 1974, was to Headquarters Eighth Air Force, Barksdale Air Force Base, Louisiana. Captain Parzianello began his tour at the Air Force Institute of Technology in June 1977.

Permanent Address: 7260 Calhoun  
Dearborn, Michigan 48126

| REPORT DOCUMENTATION PAGE   |                       | READ INSTRUCTIONS<br>BEFORE COMPLETING FORM   |
|---|-----------------------|---|
| 1. REPORT NUMBER<br>AFIT/GEP/PH/78D-9   | 2. GOVT ACCESSION NO. | 3. RECIPIENT'S CATALOG NUMBER   |
| 4. TITLE (and Subtitle)<br>DEPTH-RESOLVED CATHODOLUMINESCENCE OF<br>CARBON IMPLANTED GALLIUM ARSENIDE   |                       | 5. TYPE OF REPORT & PERIOD COVERED<br>MS Thesis   |
| 7. AUTHOR(s)<br>LUCIANO V. PARZIANELLO<br>Captain USAF  |                       | 6. PERFORMING ORG. REPORT NUMBER  |
| 9. PERFORMING ORGANIZATION NAME AND ADDRESS<br>Air Force Institute of Technology (AFIT/EN)<br>Wright-Patterson AFB, Ohio 45433  |                       | 8. CONTRACT OR GRANT NUMBER(s)  |
| 11. CONTROLLING OFFICE NAME AND ADDRESS<br>Air Force Avionics Laboratory (AFAL/DHR)<br>Wright-Patterson AFB, Ohio 45433   |                       | 10. PROGRAM ELEMENT, PROJECT, TASK<br>AREA & WORK UNIT NUMBERS<br>Project No. 2306<br>Work Unit No. R2-13 |
| 14. MONITORING AGENCY NAME & ADDRESS (if different from Controlling Office)   |                       | 12. REPORT DATE<br>December 1978  |
|   |                       | 13. NUMBER OF PAGES<br>56   |
|   |                       | 15. SECURITY CLASS. (of this report)<br>Unclassified  |
|   |                       | 15a. DECLASSIFICATION/DOWNGRADING<br>SCHEDULE   |
| 16. DISTRIBUTION STATEMENT (of this Report)<br>Approved for public release; distribution unlimited.   |                       |   |
| 17. DISTRIBUTION STATEMENT (of the abstract entered in Block 20, if different from Report)  |                       |   |
| 18. SUPPLEMENTARY NOTES<br>Approved for public release; IAW AFR 190-17<br><br>JOSEPH P. HIPPS, Major, USAF<br>Director of Information   |                       |   |
| 19. KEY WORDS (Continue on reverse side if necessary and identify by block number)<br>Gallium Arsenide<br>Carbon<br>Cathodoluminescence<br>Ion Implantation   |                       |   |
| 20. ABSTRACT (Continue on reverse side if necessary and identify by block number)<br>Three samples of VPE GaAs grown on SI Cr compensated substrate were examined by depth resolved cathodoluminescence using electron beam energies from 2.5 KeV to 15 KeV at 10° K and 39° K. The samples had been carbon-implanted, at a 120 KeV implant energy, with fluences of $10^{13}$ , $10^{14}$ and $10^{15}$ * carbon ions/cm <sup>2</sup> , respectively. The resulting cathodoluminescent spectra contained eight energy peaks: an unresolved exciton peak at 1.514 eV, a conduction band-to-carbon acceptor peak at 1.494 eV, a carbon donor-to-carbon<br>(CONTINUED ON REVERSE) |                       |   |

DD FORM 1473

1 JAN 73

EDITION OF 1 NOV 65 IS OBSOLETE

UNCLASSIFIED

SECURITY CLASSIFICATION OF THIS PAGE (When Data Entered)

sg cm  
 \* 10 to the 13th power, 10 to the 14th power and 10 to the 15th power

## BLOCK 20 (Cont'd):

acceptor peak at 1.490 eV, a possible carbon-donor-to-zinc acceptor peak at 1.487 eV, two optical phonon peaks at 1.457 eV and 1.454 eV, an unresolved As vacancy complex at 1.408 eV, and, finally, an unresolved Ga vacancy complex or As<sup>(+)</sup> Cu<sup>(=)</sup> A<sup>(+)</sup> complex at 1.361 eV.

An attempt was made to observe impurity concentration dependent energy peak shifts, of the conduction band-to-carbon acceptor and the carbon donor-to-carbon acceptor energy peaks, which had been reported for carbon implanted bulk-grown GaAs and attributed to carbon impurity banding. The failure to observe energy peak shifts in the higher-purity VPE GaAs indicates that a more probable explanation for the peak shifts observed in the bulk-grown GaAs involves the use of a tunneling-assisted transition model, which considers the combined effects of the implanted carbon impurity and the compensating impurity, Cr, present in the bulk-grown GaAs.

Finally, the cathodoluminescence spectral data was compared to the theoretical predictions of a cathodoluminescence model for GaAs developed by M. L. Cone in his Doctoral Dissertation. It was concluded that more experimental data is required to make an objective comparison.

